NCSX

Design Basis Analysis

Modular Coil CC Connection Analysis

NCSX-CALC-14-009

31 January 2008

Prepared by:

Kevin Freudenberg
Digitally signed by Kevin Freudenberg
DN: cn=Kevin Freudenberg, c=US, o=Fusion Energy, ou=ORNL, email=fdk@ornl.gov
Date: 2008.07.01 15:07:47 -04'00'

K. Freudenberg, ORNL

I have reviewed this calculation and, to my professional satisfaction, it is properly performed and correct. I concur with analysis methodology and inputs and with the reasonableness of the results and their interpretation.

Reviewed by:

David Williamson
2008.07.02 08:33:27 -04'00'

D. Williamson, ORNL Engineer

Table Of Contents

Table Of Figures

1. Executive Summary

A structural analysis of the NCSX Modular Coil (MC) C to C connection is presented. The other three interfaces have been dealt with in the previous two FDR's (bolted joint and welding) [1,2]. The analysis is based on an evolutional global ANSYS [3] model of the A-B-C half-field period [4], and detailed models of the so-called Type-1 (through-hole) & Type-2 (tapped-hole) bolted joints used to secure these flanged connections. An effective stiffness of each bolted joint type is determined and incorporated into the global model with equivalent beam elements. Various levels of friction are analyzed and the resulting bolt shear force and interface slip distributions are presented. The detailed models are also used to determine the stress range in the bolts from EM load cycles. From the previous report [1], Type 1 joint shear loads should not exceed ~15 kip, while the Type 2 joint shear loads should not exceed ~9 kip for a 100,000 cycle design life.

The CC Connection examines the outboard bolted joint using 12 additional (for a total of 44) 1.375" bolts on the inboard side of the coil to impart the shear load and deflection. A mock-up access study has shown that all 12 bolts are able to be installed. These bolts reduce the sliding deflection on inner leg significantly (from 0.02" to less than .004"). but are not able to address the extreme inner region

The inner unbolted region, which is unreachable doing assembly and where there is little available area is also examined. The current design uses pucks that have a high friction electrical insulting coating, to impart the compressive loading in this region. These pucks will be captured loosely by a shim plate that is thinner than the pucks and thus not capable of carrying compression. Further, this capture plate will be fastened to one of CC flanges by several studs. Analysis examines this design from a variety of frictional standpoints and connection possibilities given that parts are loose and may (if they slide) ride up against one another. One possibility examines the effect if the pucks are frictionless and do not carry any shear. This is critical to the first bolt since it would have to impart the shear form the unbolted region. Analysis shows that even if the inner area slips, these first bolts are always "stuck" and thus no shear is transferred to the bolt. The studs that connect the carrier plate to the flange experience around 18 ksi from the stretching of the C casting flange relative to the carrier plate. This suggests that loose fitting studs is preferable to tight fitting studs and thus, slotted holes are used near the studs to prevent the studs from experiencing any significant stress. When considering friction (mu = 0.4) under the compressive pucks, several of the puck do slip by around 0.003 inches but the pucks closest to the mid-plane always remain "stuck" and are able to handle the shear lad accrued by the slipping pucks even when the studs are not present. The peak compressive stress on the pucks is around 20 ksi which is under the allowable for 316 L stainless (39.5 ksi). Thus the inner unbolted region including carrier plate and pucks can accommodate the compression load through the pucks and will not slip out doing operation. Further, the slotted holes near the studs will ensure that the studs will not see significant stresses to due flange deformation or shear from puck slippage.

2. Introduction

The function of the NCSX modular coil system is 1) to provide specified quasi-axisymmetric magnetic field configurations, 2) to provide access for tangential neutral beam injection (NBI), radio frequency (RF) heating, and diagnostics, and 3) to provide a robust mechanical structure that minimizes non-symmetric field errors. The coil set consists of three field periods with six coils per period, for a total of 18 coils. Due to stellarator symmetry, only three different coil shapes are needed to make up the complete coil set. The coils are connected electrically in three circuits according to type, and as such can produce alternate magnetic configurations by independently varying the current for each type.

The modular coils are wound onto stainless steel castings that are then bolted together to form a structural shell. As shown in Fig. 1, the winding cavity is a "tee" structure that is located on and integral with the plasma side of the shell. During operation, electromagnetic forces push the windings outward against the shell and laterally toward the "tee", so that only intermittent clamps are required for structural support.

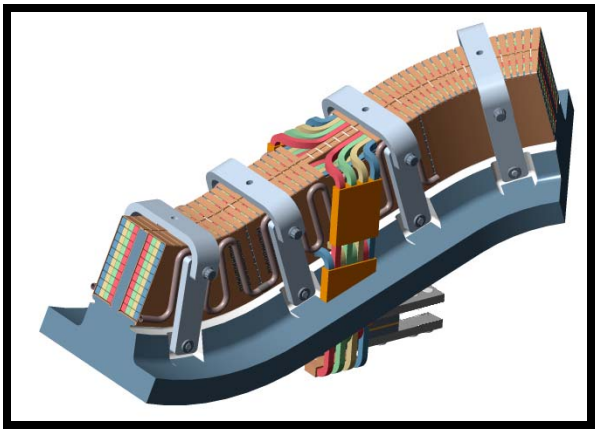

Fig. 1. Mod Coil Schematic showing the winding cavity (tee), winding and clamps

3. Analysis Approach

A CAD model of the MC half-field period assembly is shown in Fig. 2. and provides an overview of the modeling scope. This incarnation of the model represents a version of the model complete with individual shims, bolts and inner leg weld shims. This model does not depict the current inner leg shim concept, however. Fig. 3. illustrates a detailed look at the bolt/shim/flange interface on C-C flange.

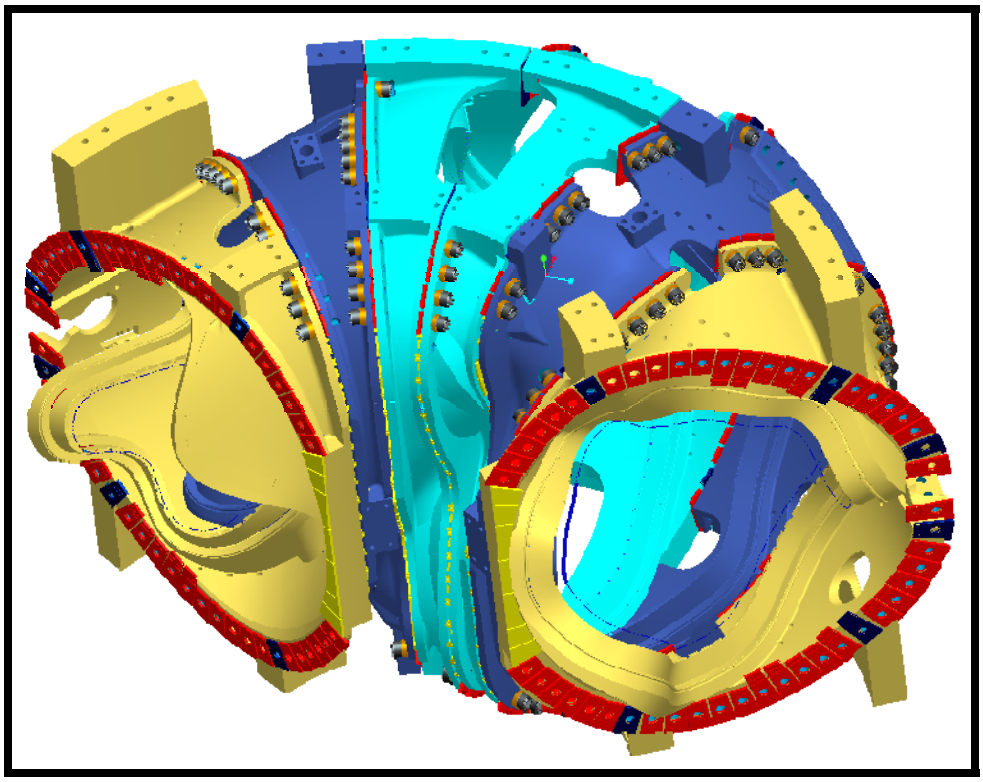

Fig. 2. Full Period Coil CAD Model (6 Coils)

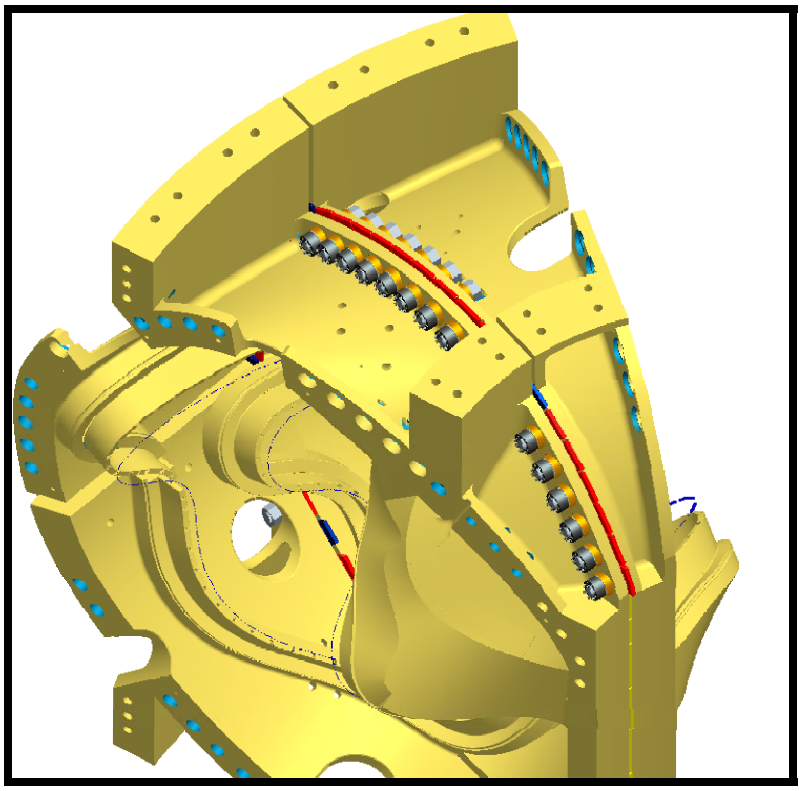

Fig. 3. C-C Interface CAD Model

3.1. Material Properties

The properties used assumed that the shell is made of stainless steel and the coil windings consist of a homogeneous copper/epoxy mixture. The properties are listed in Table 1. These values are used when the thermal loading from a localized modular coil model is applied to the shell and the winding form. Material properties for the inner shim items including studs, carrier plate and pucks are set to the "tee/shell" properties.

Table 1: Material Properties.

	E (Mpa)	CTE /K	Poisson's Ratio
Tee/shell	151,000.00	0.00E+00	0.31
Modular Coil	58,600.00	1.00E-05	0.3
Toroidal Spacer	151,000.00	0.00E+00	0.31
poloidal spacer	151,000.00	0.00E+00	0.31
Wing bag	1,100.00	2.30E-04	0.42
Wing bag	1,100.00	2.30E-04	0.32
Clamp	151,000.00	0.00E+00	0.31
Top pad	21.28	1.25E-03	0

3.2. Allowable stress (static)

Table 2 shows the minimum Stelalloy (casting) material properties defined by the NCSX team and Table 3 shows the measured weld properties of the actual casting and weld wire. These values are used to determine the maximum stress allowables for the weld and castings. Table 4 shows the property data for the 316 L stainless steel shim material [5].

Table 2: Minimum Mechanical Properties for Stelalloy

Temperature	**77K**	**293K**
Elastic Modulus	21 Msi (144.8 Gpa)	20 Msi (137.9 Gpa)
0.2% Yield Strength	72 ksi (496.4 Mpa)	30 ksi (206.8 Mpa)
Tensile Strength	95 ksi (655 Mpa)	78 ksi (537.8 Mpa)
Elongation (Casting)	32%	36%
Elongation (Weld Material)	25%	28%
Charpy V – notch Energy	35 ft. lbs. (47.4 J)	50 ft-lbs (67.8 J)

Table 3: Measured properties of Actual castings and weld wire.

updated 2/15/07

AVERAGES

Type C

Casting Compariso	77K (-320F)							293K (RT)						
Property	**Required**	**C1**	**C2**	**C3**	**C4**	**C5**	**C6**	**Required**	**C1**	**C2**	**C3**	**C4**	**C5**	**C6**
Elastic Modulus	21 Msi (144.8 Gpa)	23.3	25.5	24.9	26.5	30.2	28.8	20 Msi (137.9 Gpa)	23.1	22.7	21.6	23.1	27.3	24.1
0.2% Yield Strength	72 ksi (496.4 Mpa)	98.4	93.2	97.1	97.8	102.5	99.5	34 ksi (234.4 Mpa)	35.1	36.6	38.3	37.4	38.8	44.5
Tensile Strength	95 ksi (655 Mpa)	170.3	163.8	163.1	164.8	170.9	159.9	78 ksi (537.8 Mpa)	83.7	82.4	82.7	83.1	87.0	83.7
Elongation	32.0%	55.7%	54.3%	55.7%	54.0%	42.4%	42.3%	36.0%	52.0%	53.5%	52.5%	55.7%	58.0%	40.3%
Charpy V – notch Energy	35 ft. lbs. (47.4 J)	77.7	84.3	99.7	86.7	80.3	85.3	50 ft-lbs (67.8 J)	142.0	150.7	157.3	175.7	139.0	152.3

Type A

Casting Compariso	77K (-320F)							293K (RT)						
Property	**Required**	**A-1**	**A-2**	**A-3**	**A-4**	**A-5**	**A-6**	**Required**	**A-1**	**A-2**	**A-3**	**A-4**	**A-5**	**A-6**
Elastic Modulus	21 Msi (144.8 Gpa)	25.5	25.3	26.7	28.9	26.4	27.9	20 Msi (137.9 Gpa)	21.7	22.2	21.9	22.9	23.1	22.6
0.2% Yield Strength	72 ksi (496.4 Mpa)	97.3	99.9	98.9	100.0	101.0	103.2	34 ksi (234.4 Mpa)	36.6	43.3	43.2	43.8	42.4	44.5
Tensile Strength	95 ksi (655 Mpa)	166.3	165.3	166.0	165.9	165.2	163.0	78 ksi (537.8 Mpa)	82.4	83.7	82.6	84.6	82.2	89.2
Elongation	32.0%	56.0%	56.3%	51.0%	46.0%	48.7%	38.3%	36.0%	53.2%	56.0%	53.3%	50.3%	50.0%	49.0%
Charpy V – notch Energy	35 ft. lbs. (47.4 J)	78.7	79.0	87.3	76.7	70.3	73.0	50 ft-lbs (67.8 J)	163.7	164.0	158.0	150.3	146.3	126.7

Type B

Casting Compariso	77K (-320F)							293K (RT)						
Property	**Required**	**B-1**	**B-2**	**B-3**	**B-4**	**B-5**	**B-6**	**Required**	**B-1**	**B-2**	**B-3**	**B-4**	**B-5**	**B-6**
Elastic Modulus	21 Msi (144.8 Gpa)	25.9	27.4	29.3	25.3	29.3		20 Msi (137.9 Gpa)	22.7	22.5	22.6	22.8	22.6	
0.2% Yield Strength	72 ksi (496.4 Mpa)	98.7	103.9	107.4	100.2	107.4		34 ksi (234.4 Mpa)	43.3	58.9	42.7	42.6	42.7	
Tensile Strength	95 ksi (655 Mpa)	164.9	177.5	172.5	166.1	177.5		78 ksi (537.8 Mpa)	86.0	86.6	84.1	85.6	84.1	
Elongation	32.0%	46.3%	50.3%	56.3%	53.3%	56.3%		36.0%	47.3%	49.5%	44.7%	43.5%	44.7%	
Charpy V – notch Energy	35 ft. lbs. (47.4 J)	88.0	63.7	74.7	65.7	74.7		50 ft-lbs (67.8 J)	146.7	135.7	115.0	119.7	115.0	

Weld Material	77K (-320F)							293K (RT)							
Property	**Required**	**Lincoln 3018926/7 8309**	**Lincoln Lot # 3012668/8 2743**	**Lincoln 3018513/7 8308**	**Lincoln Lot # 3017006/7 2262**	**Metrode Lot # WO21735**	**Metrode Lot # WO19711**	**Required**	**Lincoln 3018926/7 8309 Doc #10**	**Lincoln Lot # 3012668/8 2743 see previous info --**	**Lincoln 3018513/7 8308**	**Lincoln Lot # 3017006/7 2262**	**Metrode Lot # WO21735**	**Metrode Lot # WO19711**	**Previously Reported Heat/Lot # 3012668/8 2743**
Elastic Modulus	21 Msi (144.8 Gpa)	23.3	27.1 Doc#9	27	23.2	24.3	26.4 Doc#9	20 Msi (137.9 Gpa)	24.5 Doc 10	22.6	23.4	24.9	23	23.1 Doc#10	25.5 Doc#10
0.2% Yield Strength	72 ksi (496.4 Mpa)	114.3	126.3 Doc#9	128.2	112.4	102.1	109.5 Doc#9	34 ksi (234.4 Mpa)	56.9 Doc #10	57.4	65.2	54.9	54.8	63.9 Doc#10	56.5 Doc#10
Tensile Strength	95 ksi (655 Mpa)	157.5	187.7 Doc#9	182.1	176.4	166.6	166.9 Doc#9	78 ksi (537.8 Mpa)	93.9 Doc #10	93.7	95.2	92.1	88.2	98.1 Doc#10	85 Doc#10
Elongation	32%	16.0%	33% Doc#9	34.0%	48.0%	38.0%	34% Doc#9	36.0%	42% Doc #10	41.5%	38.0%	42.5%	37.5%	54% Doc#10	55% Doc#10
Charpy V – notch Energy	35 ft. lbs. (47.4 J)	36.33	51 Doc#11	54	53	48	48 Doc#11	50 ft-lbs (67.8 J)	100 Doc #10	98	103	117	93	111 Doc#12	102 Doc#12

Table 4: Low temperature property data for 316L and 31LN stainless steel. (Vogt)

Table I. Chemical Composition

Steel	C	N	Mn	Si	S	P	Ni	Cr	Mo	Al	B
316L	0.024	0.033	1.601	0.530	0.013	0.010	13.58	17.40	2.139	0.006	0.0025
316LN	0.023	0.235	1.518	0.534	0.012	<0.01	13.69	17.22	2.223	0.007	0.0018

Table II. Mechanical Characteristics of the Steels at 77 and 300 K

	Temperature (K)	σ_y (MPa)	σ_u (MPa)	A (Pct)	S (Pct)
316L	300	262	574	56.4	75.9
	77	402	1156	56.8	69.6
316LN	300	328	697	47.3	71.7
	77	902	1415	45.6	63.7

Per the NCSX Structural Design Criteria [6], Sm shall be the lesser of 1/3 of the ultimate strength or 2/3 of the yield strength at temperature. Since the weld region includes the Stelalloy casting, weld metal, HAZ, and shims made of 316-L, the strength values shall be the lesser of these. Thus for the shim and the pucks, the allowable yield strength is 58 ksi and 2/3 of yield = 39 ksi for the peak membrane stress. The weld data shows that the lowest ultimate strength is 157.5 for the weld wire. A "knock down" factor of 0.45 is applied, since it is a fillet weld joint and, therefore, Sm=0.45 * 157.5 / 3 = 24 ks for the welds. Peak stresses, such as those caused by geometric discontinues (corners, holes) have an allowable range up to 1.5*Sm per the design criteria. Fatigue will be addressed in a section 6 below. Table 5 indicates the allowable membrane stress for each component in the flange to flange weld connection. **Note:** The weld numbers are for fillet welds and the studs welds do not require the 0.45 factor.

Table 5: Allowable stress (Sm) for the flange connection components

Item	Material	Allowable Sm (ksi)
shim	316L	39
weld	Lincoln Weld Wire	24
casting flanges	Stellalloy	54
compressive pucks	316L	39

3.3 Magnetic Loading

Calculations to determine the fields and forces acting on all of the stellarator core magnets have been completed for seven reference operating scenarios. The worst case for determining forces in the modular coils appears to be the 2T high beta scenario at time=0.197-s. Two independent field calculations have been performed, one with the ANSYS code and the other with MAGFOR [7]. A comparison of magnetic flux density at 2-T indicates that the models are in good agreement, with only a 4% difference in peak field due primarily to mesh and integration differences.

3.4. Assumptions

The non-linear (frictional) analysis of this structure is based on the half-field period model shown in Fig. 4. Structural continuity between adjacent coils is handled two different ways to accommodate the computational limitations of this large problem:

1. At one particular interface (in this case CC), pipe elements with appropriate section properties are used to represent the characteristics of a bolted interface (see Attachment Section 4.1). Contact

elements at this interface are allowed sliding contact (no separation). Fig. 5 shows the pipe elements used to model the bolt, connecting it to the hole via bar elements.

2. The other bolted interfaces are modeled with "Bonded Contact."

This un-bonded, sliding-only contact surface modeling approach seems to be the only way to get the analysis to complete in a reasonable amount of time (of order 12 hours). When the more general contact behavior is implemented (stick-slip, open-closed), the model takes four days to reach 4% of the EM load case. The simplified approach is decent, with frictional shear only developing when a positive normal pressure occurs. So, shear loads in the bolts are reasonably accurate. However, since this approach simulates a "hooked" interface, it does not accurately represent the change in axial load on the bolts.

Simulating the 18-coil MC system with a half-field period (3-coil) model requires the application of displacement U(R,θ,Z) constraint equations (CE) to the cut boundaries (θ=0º & 60º). Nodes on these symmetry planes are rotated into a cylindrical coordinate system. Fig. 6 shows a graphical representation of this boundary condition which illustrates the following general rule. The vertical lines represent the link between the +Z nodes and -Z nodes. One node on the B shell is restrained in the vertical direction (z) to complete the required DOF constraints.

$$UR(R,\theta,Z) = +UR(R,\theta,-Z)$$
$$U\theta(R,\theta,Z) = -U\theta(R,\theta,-Z)$$
$$UZ(R,\theta,Z) = -UZ(R,\theta,-Z)$$

The electromagnetic loading (EM) is limited to one particular time-point (t=0.0s) within one particular current scenario (2T High-β). It is commonly thought that this represents the worst load case. However, there has been no attempt to verify this position. The nodal force files for each coil are read into the structural routine before the solution. Fig. 7 shows a plot of the coils and nodal force vectors (for visualization purposes).

Previous analysis [4,8] has shown that the non-linear contact interactions between the coils and winding forms do have an impact on stress. Running a non-linear sliding winding in this case is computationally difficult given the compute time required. Thus, to simulate this effect in a linear manner, a "wimpy" winding pack was used in these models. It has a modulus of 856 Mpa or 100 times less than that listed in Table 1. This allows for the brunt of the magnetic loading to transfer directly to the tee as the winding pack stiffness is reduced. This has a greater effect near the tee region than the flange interfaces but to be conservative, the value was used to simulate the maximum amount of magnetic loading the shell would ever experience.

Contact Stiffness

Following the presentation of numerous global model results which showed high shear loads in some of the bolts, a detailed review of the contact element characteristics uncovered a defect in the model. The default contact element shear stiffness (~0.17E11 N/m^3) was found to be too soft, and flange faces slipped when

they should have been stuck. Over-riding the default shear stiffness value with incremental increases produced lower bolt shear loads and longer computer run-times for the representative A-A interface. This characteristic is shown in Fig. 2.0-6. A shear stiffness of 5E11 N/m^3 seems to provide a reasonable compromise in accuracy and run-time. All analyses presented here use this value which is ~30x larger than the default stiffness. However, when considering the CC added inner bolts, even the value of 5e11 N/m^3 is too small and larger values are used.

3.5. Special Considerations/assumptions for the unbolted region of CC.

In all cases, the pucks are bonded to the carrier plate. The carrier plate is bonded to the studs and the studs are bonded to the flange of one of the C coils. The pucks are the same size as the holes in the carrier plate in order to allow the solution to converge when puck sliding is allowed. The carrier plate is also 0.5" thick instead of the 7/16" design allocation but it still cannot carry compression since it has no contact elements associated between it and the mating CC flanges. Also, the surface condition whether bonded, frictional or frictionless may occur on both or one side of the shim at the same time. Thus, shear could be transmitted to the carrier plate if only one side slips.

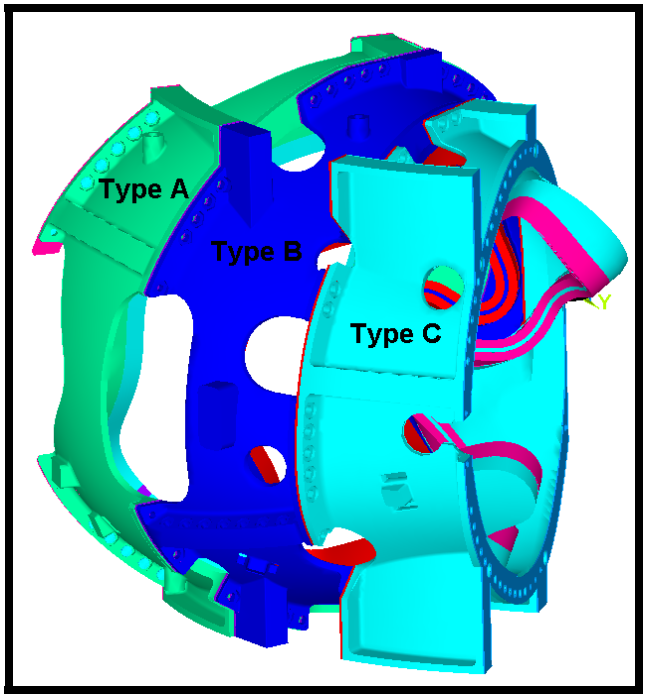

Fig. 4. Half-Field Period Global ANSYS Model.

Model Boundaries in a cylindrical coordinate system are at:
θ=0º (mid-thickness A-A shim)
θ=60º (mid-thickness C-C shim)

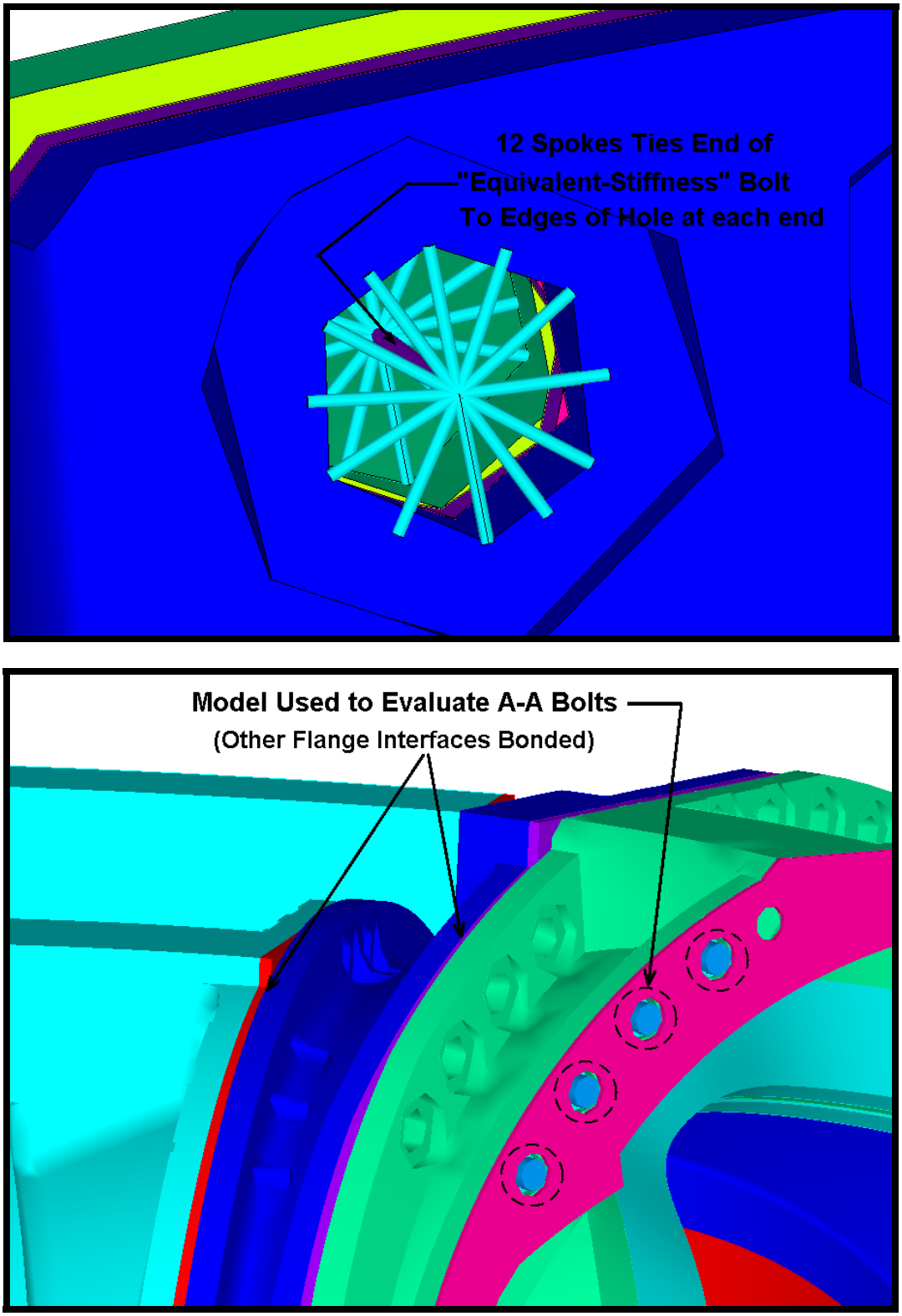

Fig. 5. Pipe Elements with Appropriate Section Properties Used to Simulated Bolted Connection Equivalent Pipe Elements Tie A-B Flanges (diameters scaled for visualization purposes)

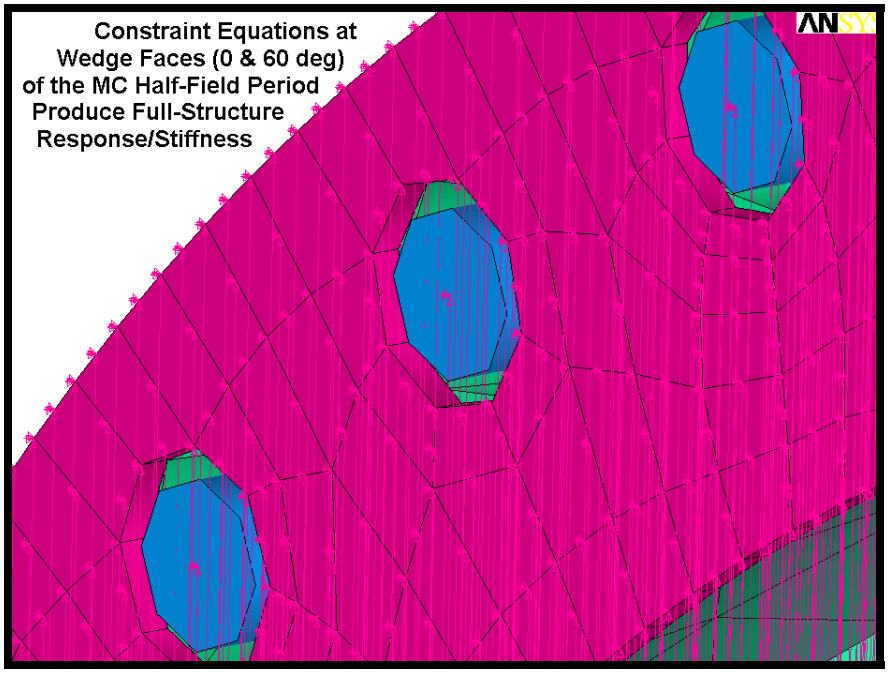

Fig. 6. Constraint Equation Symbols at A-A Shim Mid-Thickness

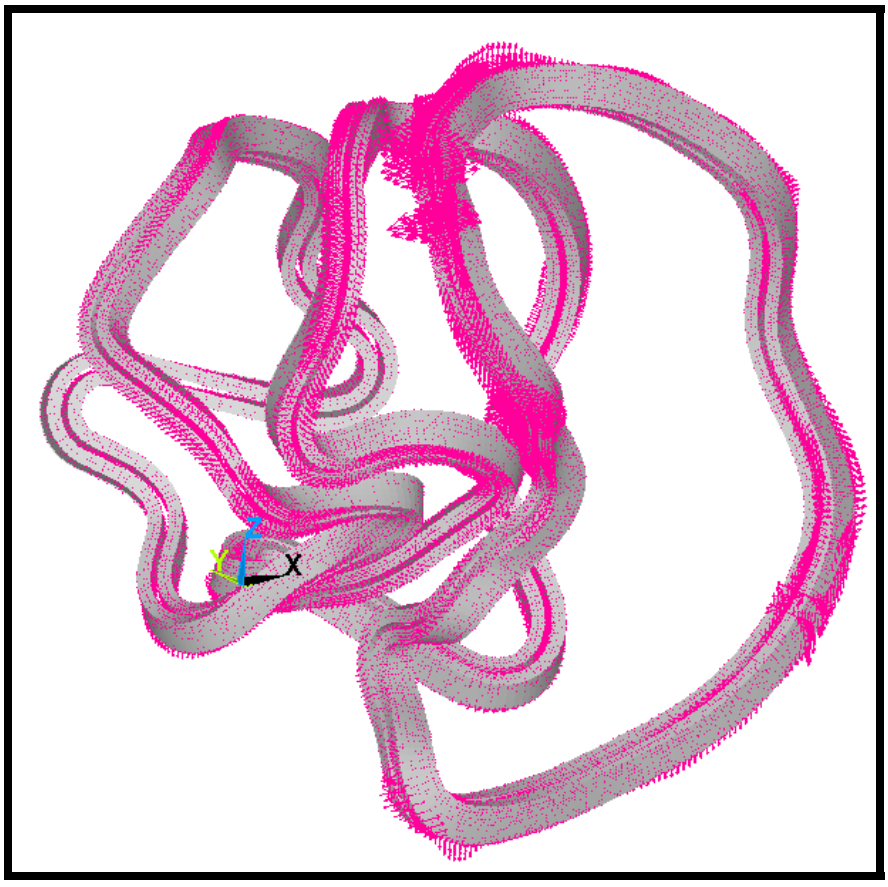

Fig. 7. Nodal Forces (t=0.0s of 2T, High-β)

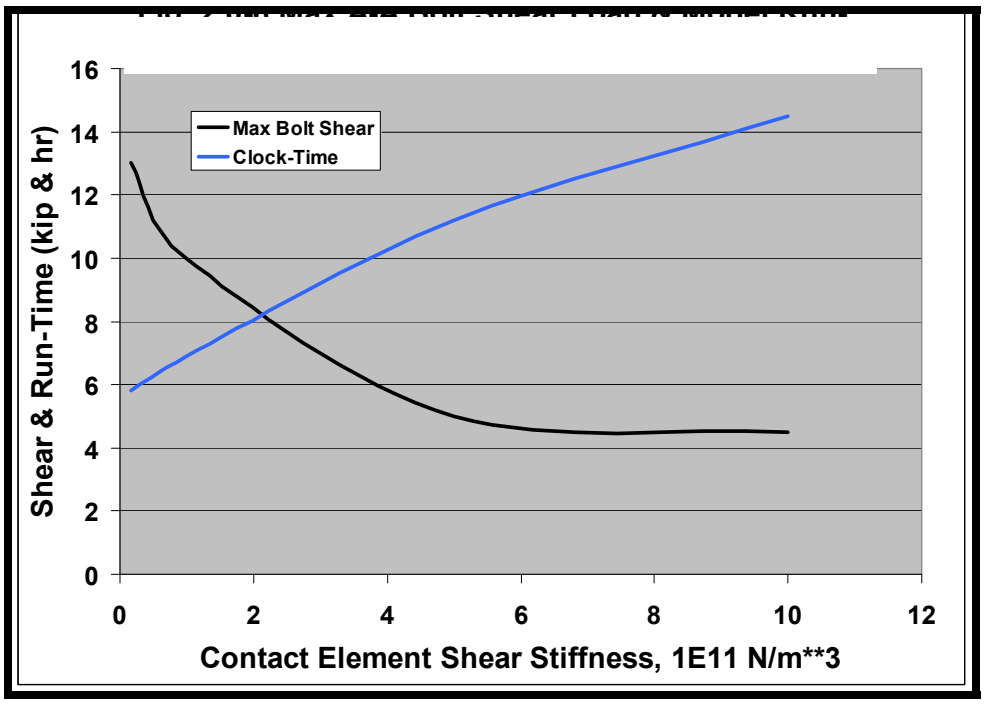

Fig. 8. Max A-A Bolt Shear Load & Model Run-Time vs Contact Stiffness

4. Global Model Results

4.1 Bolted Interfaces with Friction -original design - no inboard bolts added

Various analyses have indicated the need to improve structural continuity in the inboard leg region of the MC system. Designers have responded by modifications which include the addition of inboard leg bolts at A-A, A-B & B-C. The global model is exercised in an effort to quantify the shear load on the bolts.

Fig. 9 shows a bar chart of the tensile preload and transverse shear load form the EM load application in each of the 32 original C-C bolts, and a model plot showing the bolt numbering system. The bolts are preloaded to roughly 75 kip (kilo-pounds), and the flange and shim surfaces have a finish which produces a design-basis friction coefficient of 0.4. Bolt numbers 1 & 32 carry the largest shear force at < 3 kips. This is indicative of the bolts being stuck and the loading transferred through friction as expected. A higher contact stiffness would reduce the residual shear load that the bolts experience. This is discussed in more detail below in Appendix A.1

Fig. 10 shows a contour plot of the C-C interface slippage (in meters) and the contact status plot bolt shear load vectors as a result of the EM load application. The blue regions of the contour plot are limited to the areas where bolts pull the flanges together and indicate little or no slippage. The slippage away from the inboard leg is quite small (< 0.05 mm).

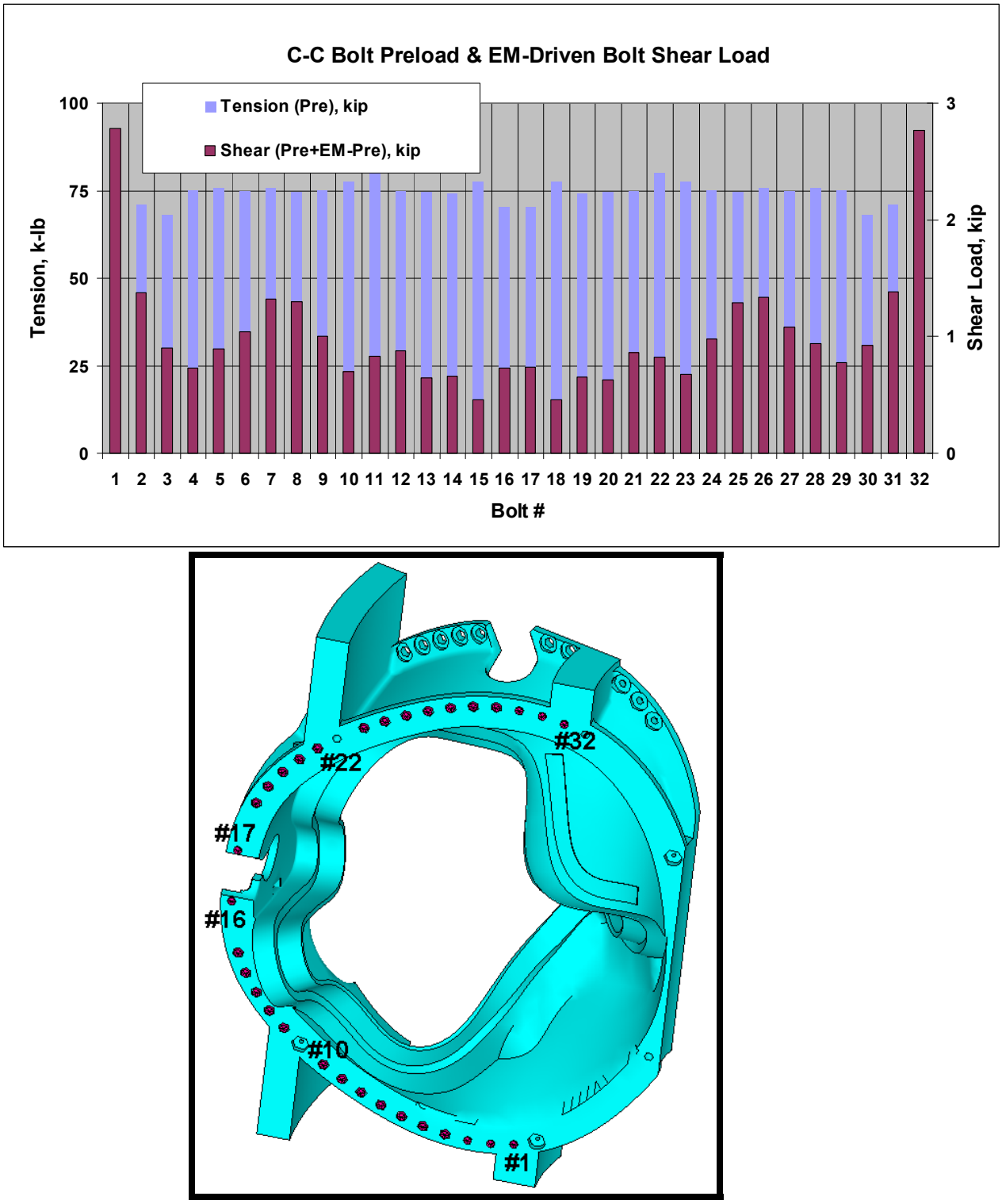

Fig. 9. C-C Bolt Preload & EM-Driven Shear Load (top) & Bolt Numbering (bottom)

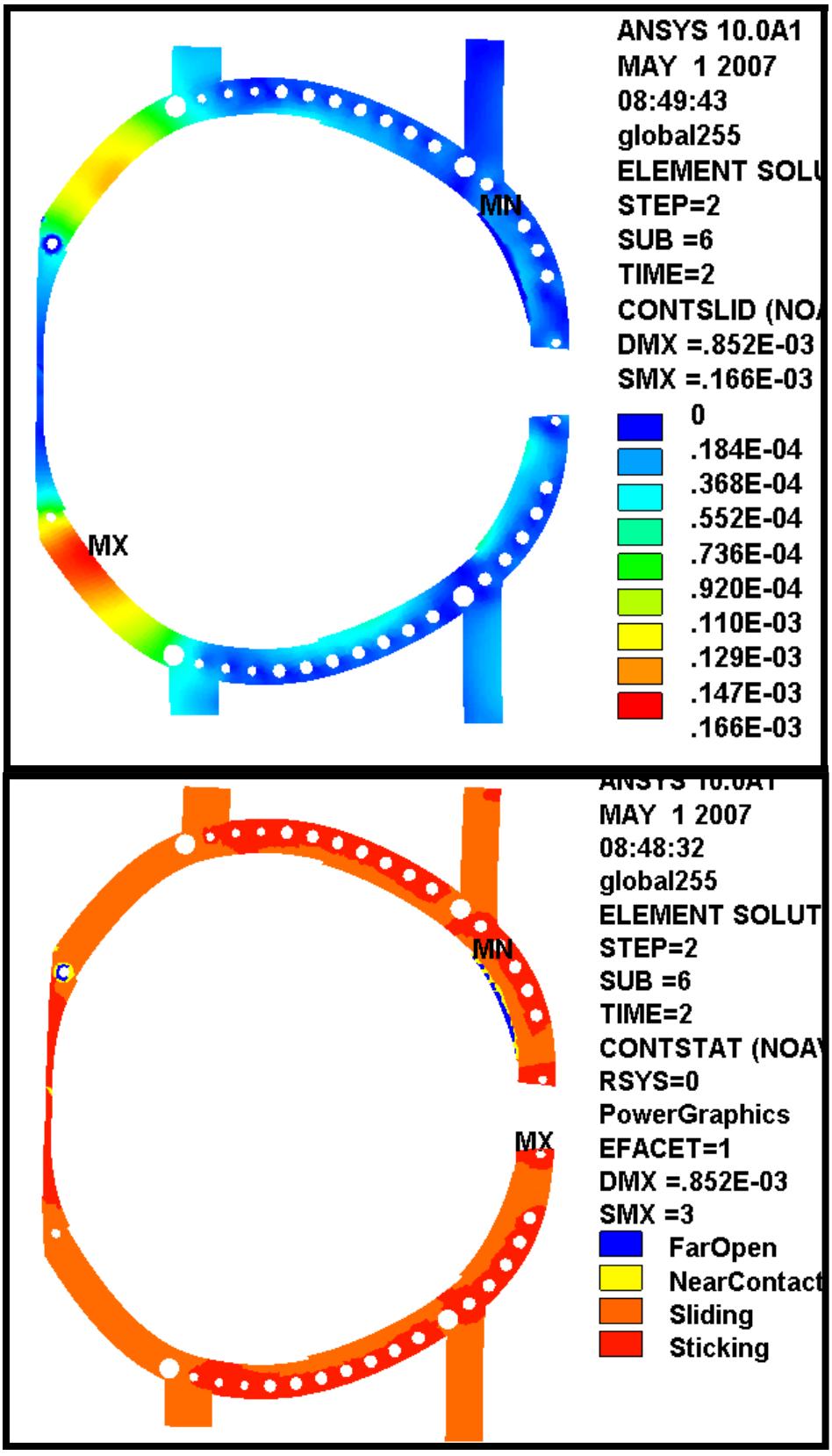

Fig. 10. C-C Slip [m] & Bolt Shear Loads [kip] from EM Load Application

4.2. Case Study 1> Results for the various CC inner leg options

The inner leg of the CC coil cannot be welded together like the other interfaces because of the electrical break isolation requirement. As such, the inner leg is outfitted with 12 inner bolts. These bolts are 1.375" diameter, which are same diameter as the outer bolts. The number of bolts was chosen based on the positive results form an access study on a full scale mock up. These bolts are shown in Figure 11.

Fig. 12. shows a bar chart of the tensile preload and transverse shear load from the EM load application in each of the C-C bolts and a model plot of the friction scheme for the run. Here, 6 bolts have been added to the CC even though there are holes present for all 12. The additional holes (6 inner most holes indicated by x's) simply do not have any bar/pipe elements connecting them. The bolts are preloaded to roughly 75 kip (kilo-pounds), and the flange and shim surfaces have a finish which produces a design-basis friction coefficient of 0.4 under all of the bolts. The unbolted area on the extreme inboard has friction set to 0.04 friction. In further analysis the inboard friction is also set to 0.4. which allows for a bounding range for slippage. Fig 13 illustrates the sliding and contact behavior on the CC interface. A similar series of plots is included for the case of adding twelve bolts instead of six (Fig. 14 - Fig. 15).

Table 3 shows a summary of the max slip and shear loading from the set of analyses All of the outboard bolts have very low shear (<1.5 kip). This is indicative of the bolts being stuck and the loading transferred through friction as expected. Some of the inner leg bolts see higher shear (approx 5 Kips) but these bolts see little to no motion under them. This discrepancy is related to the contact stiffness problem defined above in section 3.4. The shear loads are most likely high by at least a factor of 2. Appendix 2 examines the inner leg of CC using 1.5" bolts and looks at a range of contact stiffness. The shear values drop by at least half on the inboard bolts as the stiffness increased by 10X. Larger bolts are used in the appendix because the added preload was thought to be beneficial from a shear load standpoint. However, the cost of the tooling required to achieve the 1.5" diameter threads is prohibitive. Also, given that the shear loads are overestimated due to the contact stiffness and that the bolts can withstand up to 8 Kips of shear from a fatigue standpoint, all of the inboard bolts and outboard bolts are stuck and friction is able to transfer the shear. These bolts do experience some minimal residual shear form flange/flange deformation and typically this is under 1 Kip. Although the low contact stiffness value causes an overestimate of bolt shear it has a minimal effect on sliding.

All of the analysis on the CC joint, or any of the other joints, has always considered perfect fit up. To check this behavior, a 0.005" gap was instituted, (using an ANSYS contact element keyopt option), between the flange and the shim. The results for bolt load and shim are shown in Fig 22 which indicates that the effect of the gap is minimal. The max slippage still occurs in the same area after the coil has compressed down onto the flange. The inner leg with the gap has standard contact behavior so that it can close as opposed to the sliding behavior of the areas around the bolts.

Table 3: Max slippage and peak shear of the inboard bolts

Inboard Friction	# of inboard bolts	Max sliding distance (in)	Max Shear Force (kips)
0.4	0	0.0065	2.8
0.4	6	0.0047	2.4
0.4	12	0.0011	2.7
0.04	0	0.0199	4.9
0.04	6	0.0143	4.5
0.04	12	0.0024	3.5
Imperfect Fit-up gap of .005" on unbolted region	0	0.0193*	3.3

*sliding occurs after gap has closed

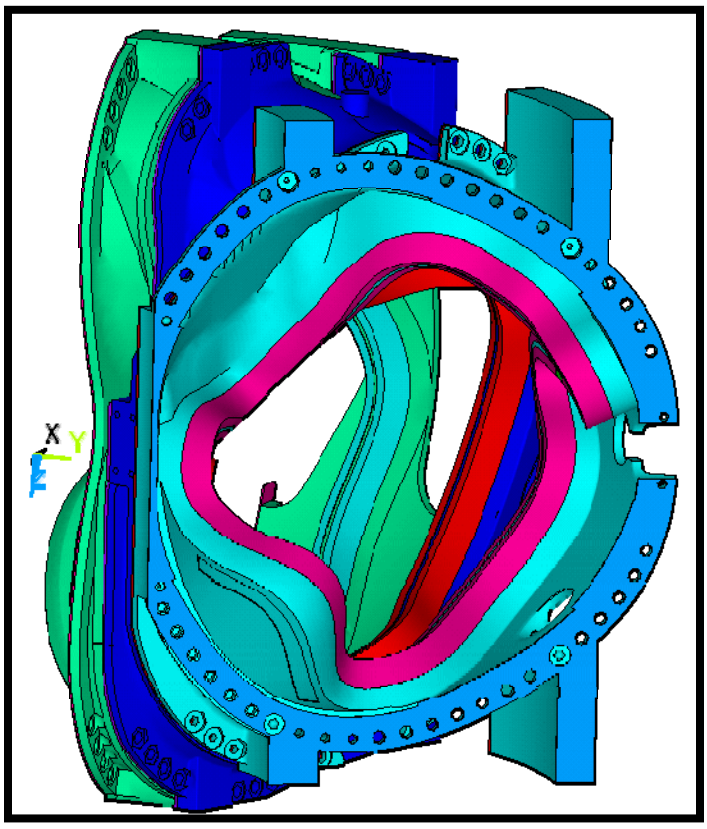

Fig. 11. Maximum added C-C bolt holes

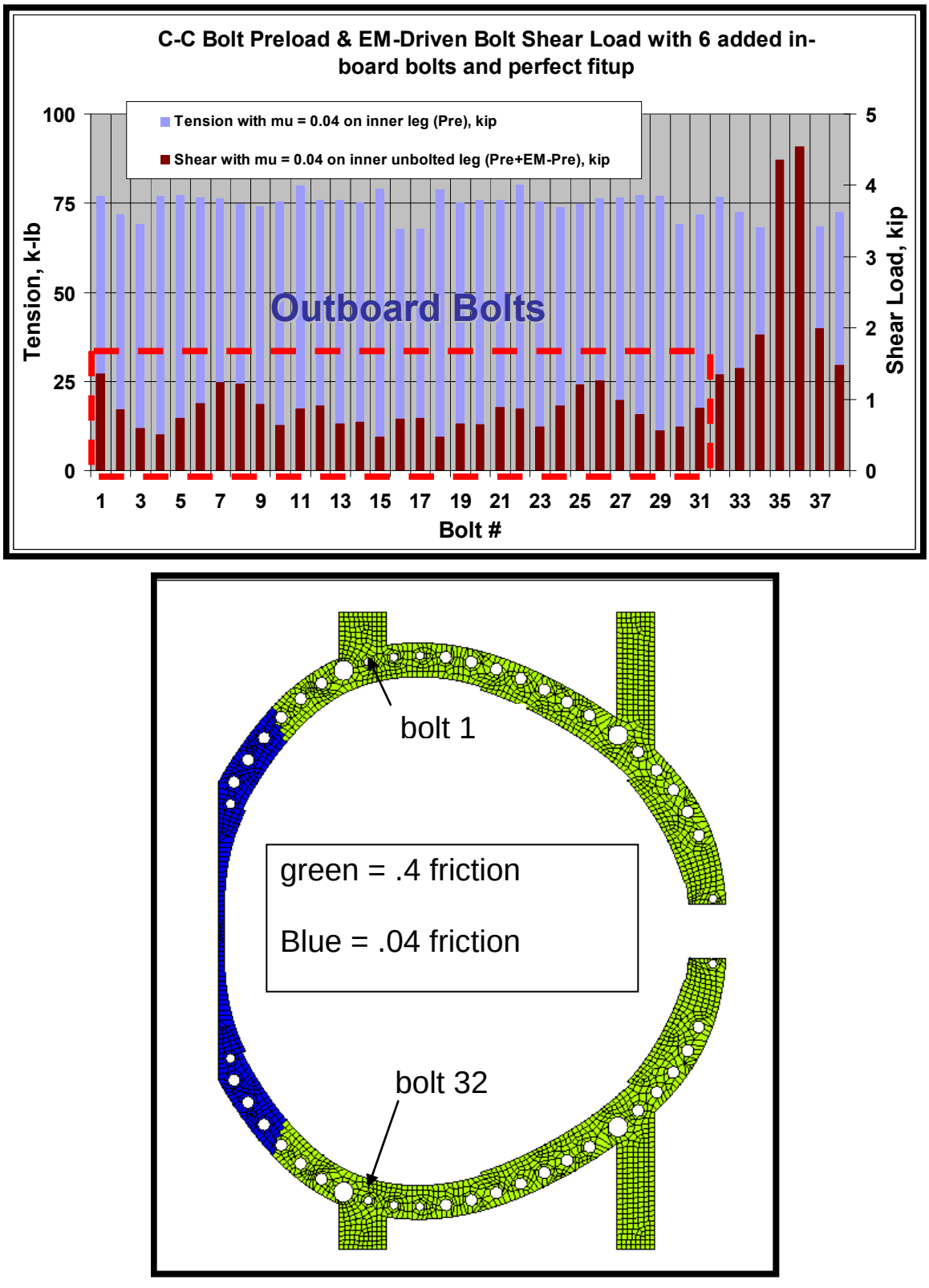

Fig. 12. C-C Bolt Preload & EM-Driven Shear Load (top) & Friction scheme [6 added in board bolts]

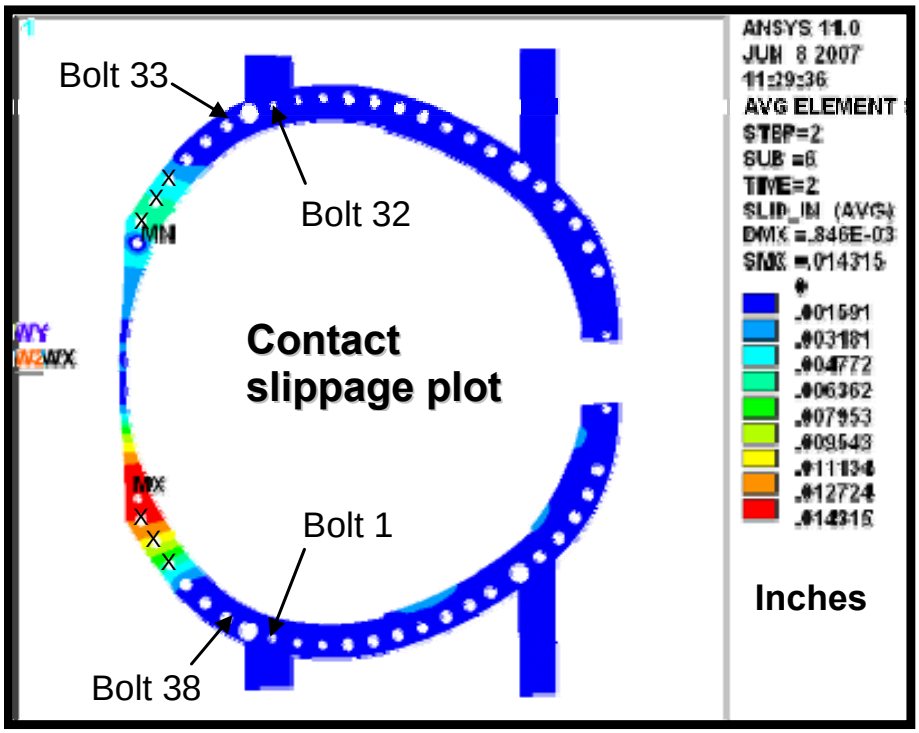

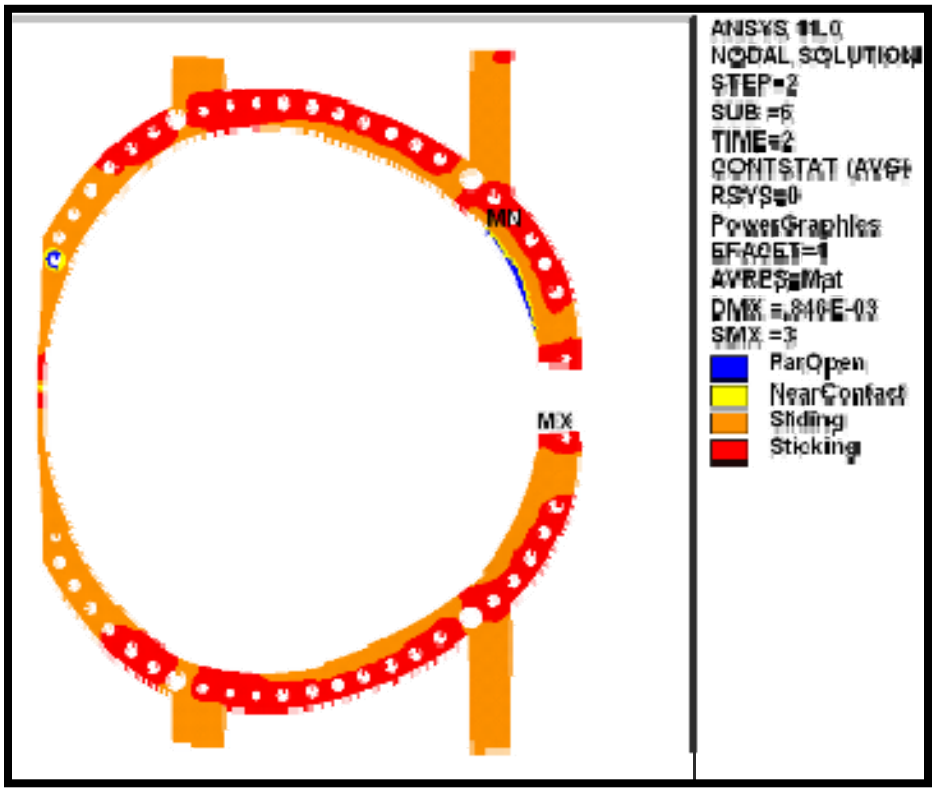

Fig. 13. C-C Slip [m] & Bolt Shear Loads [kip] from EM Load Application [6 added in board bolts]

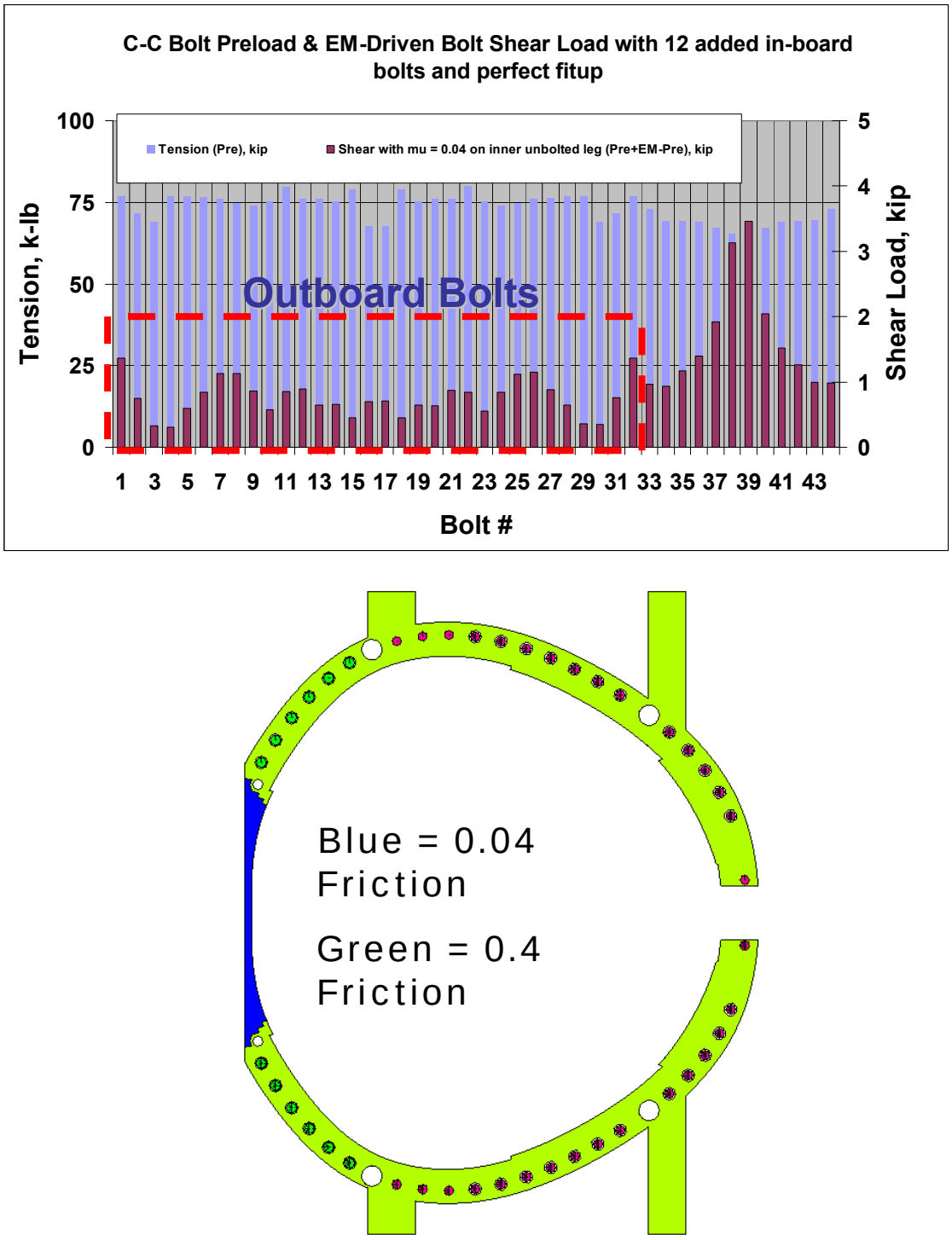

Fig. 14. C-C Bolt Preload & EM-Driven Shear Load (top) & Friction scheme [12 added in board bolts]

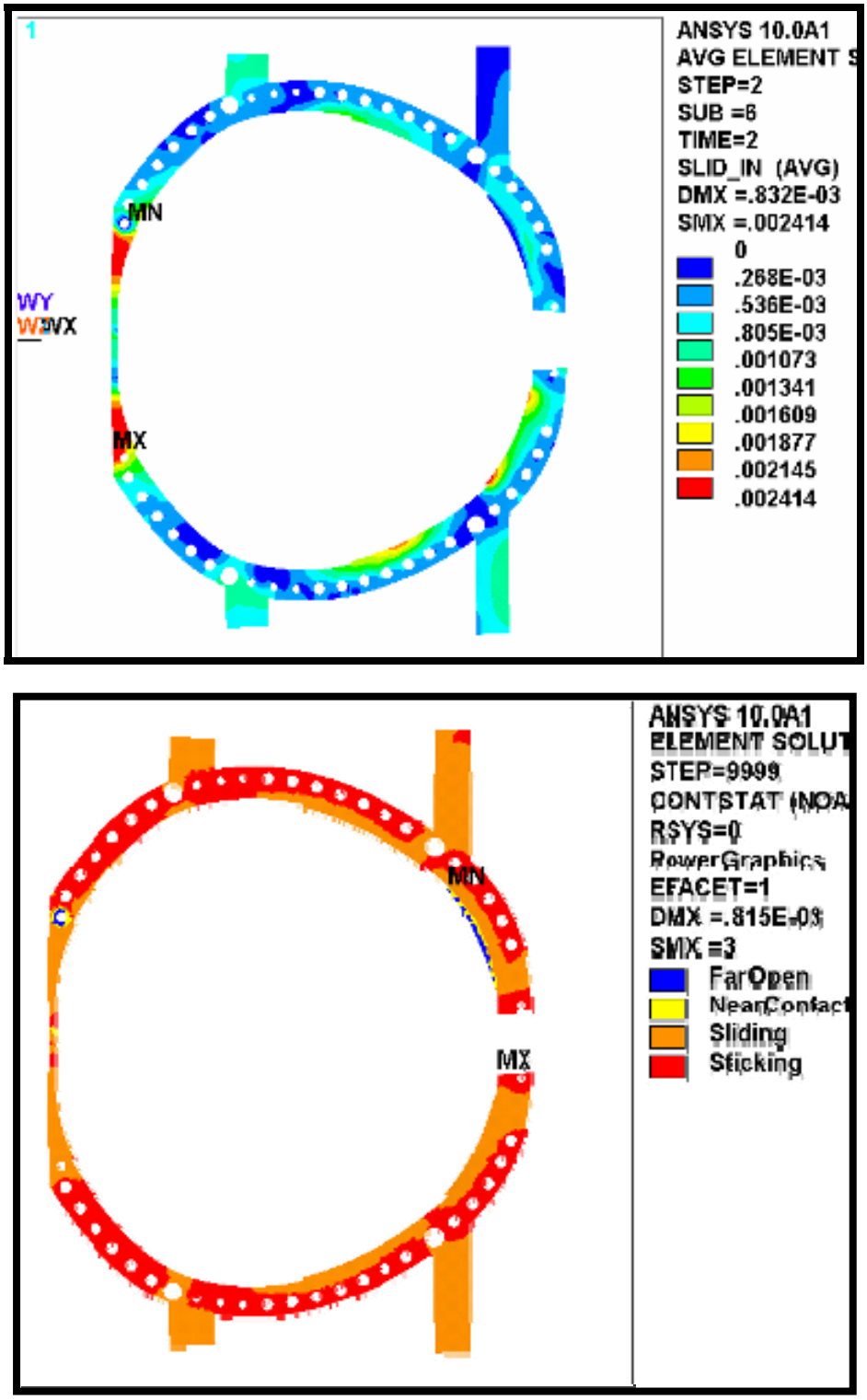

Fig. 15. C-C Slip [m] & Bolt Shear Loads [kip] from EM Load Application [12 added in board bolts]

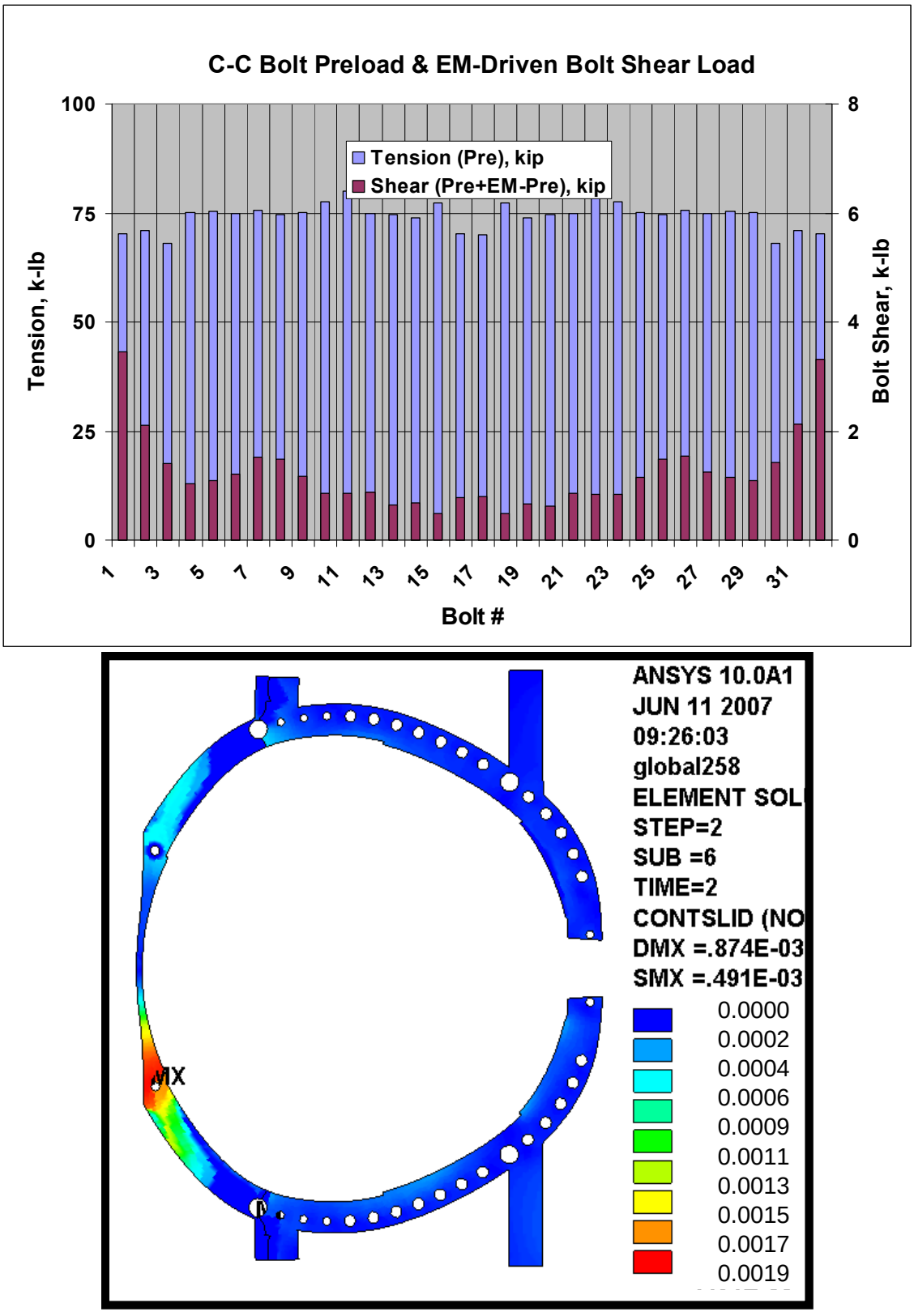

Fig. 16. C-C Slip [m] & Bolt Shear Loads [kip] and slippage (in)from EM Load Application [imperfect fit-up of .005" between flange and shim.

4.3. Unbolted C-C inner leg region.

In general, having loose fitting parts is a challenge to model and analyze and thus, a limiting contact approach is adopted. The analysis basically uses in all or nothing approach when considering contact between the pucks and studs to the carrier plate. The unbolted region of the C-C joint is shown below in Figure 17. The puck carrier is shown as green while the studs and pucks are shown as orange and red respectively. The image shows the initial design of using two oblong style studs to retain the carrier plate. This has changed in latter versions to three rounds studs which will be welded into the flange. The design calls for the pucks to be smaller than the holes in the plate so that the carrier plate acts as a positioning fixture during assembly. However, the analysis cannot accommodate this as the pucks would be free bodies inside the carrier plate and convergence could not be accomplished. Thus, the pucks are bonded to the carrier plate which is conservative as it treats the puck as having wandered over to the edge of the plate This could transmit shear to the carrier plate and to the studs if one side of the puck slipped. The pucks will be coated on all sides with the same high friction alumina coating that is used on the outboard shims. A friction coefficient of 0.4 is used for the interface between the pucks and the flange unless that interface has been set to slip (mu = 0) in certain runs. The carrier plate is also 0.5" thick instead of the 7/16" design allocation but it still cannot carry compression since it has no contact elements associated between it and the mating CC flanges.

Appendix B shows some of the earlier work on determining the shear and compression loading on the inboard leg from the previous analysis [4,8]. The figures show that the largest compressive force on the CC flange occurs near the midplane on the inboard flange face. Further, there is some shear (both radial and vertical present on the flange face near the midplane as well.

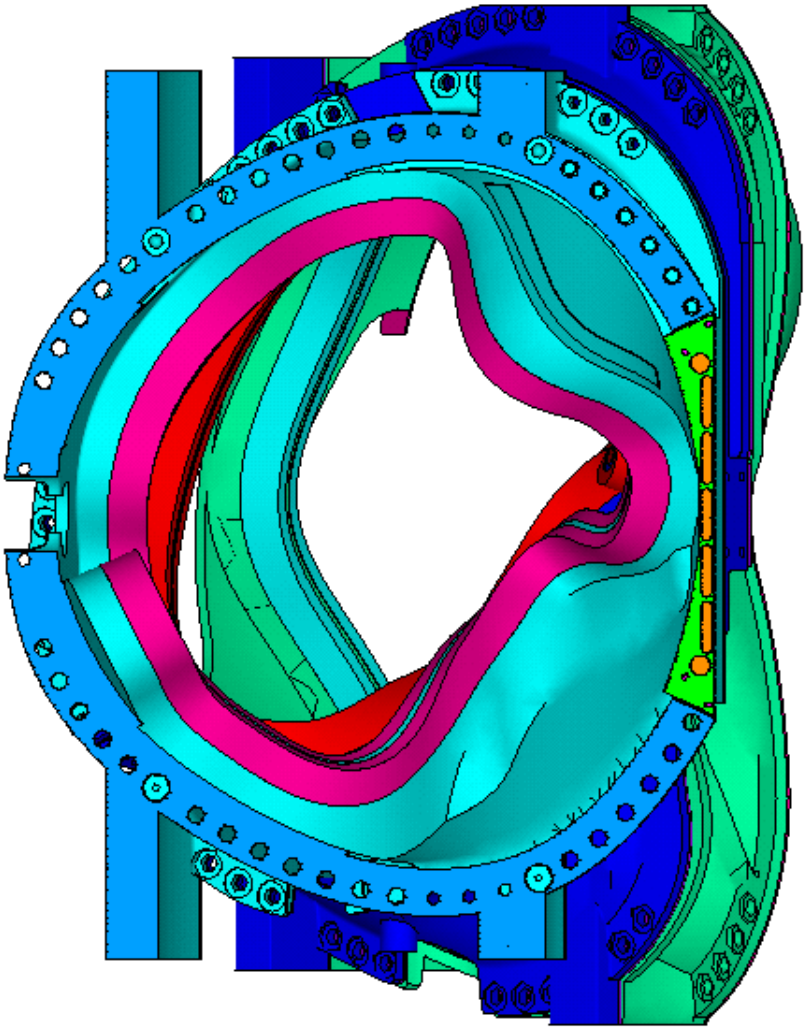

Figure 17. CC unbolted inner leg region including bolts on outer leg.

Case #1: bolts on outboard leg and frictionless pucks

The first step in analyzing the outboard leg is to verify again that no matter what design is chosen for the unbolted region, the outboard leg bolts will not slip. Thus, the original oblong stud model was run with bolts (instead of simple bonding the outboard leg) and a frictionless condition under the compression puck. This would give the greatest amount of flexibility to the inner region which could impact the bolt performance.

Figure 18 shows the now familiar bolt preload chart and shows that all shear loads on the bolts are low and are indicative of a "no slip" condition around the bolts. The inner region bolt preload was slightly underestimated during this run but an increase in compression only strengths the case that the bolts will not slip. Figure 19 verifies that there is no slip under the bolts and the friction is enough to prevent motion. Thus, the outboard bolts are unaffected by the inner leg as long as it carries compression.

Figure 20 shows the stress intensity of the main components of the inner shim. The peak compression stress on the pucks is around 20 ksi and under the allowable for compression on 316 L (of 39.5 ksi). Further the stresses on the carrier and the studs are also under this limit. However, the studs are actually round are not oblong, which increases their effective area and thus stress on the round studs will be higher than shown here. The primary purpose of this run was to determine the behavior of the outboard bolts for this concept.

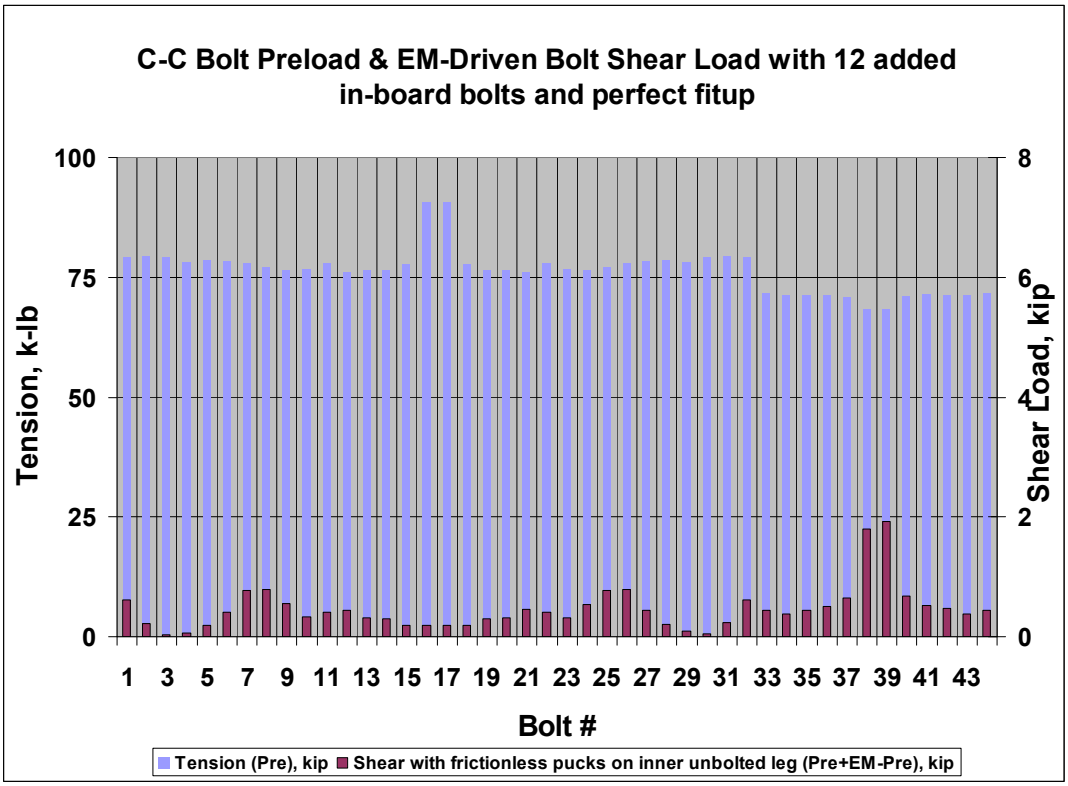

Fig. 18. C-C Bolt Preload & EM-Driven Shear Load (top) & Friction scheme with inner leg pucks

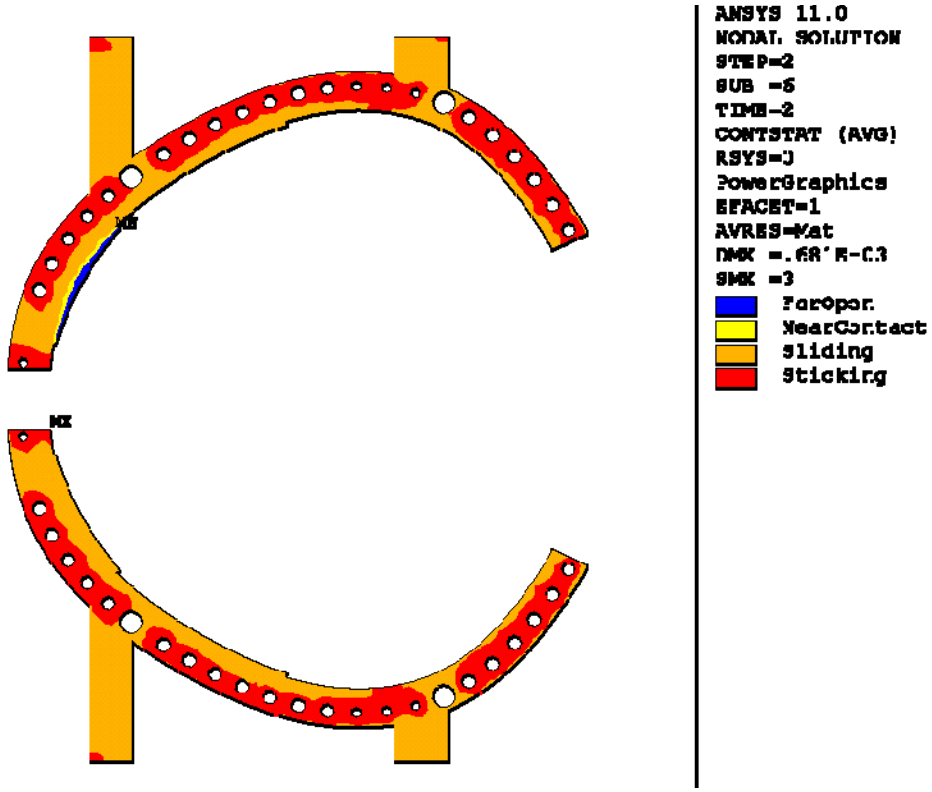

Fig. 19. C-C Contact plot of outboard bolts with inner leg pucks.

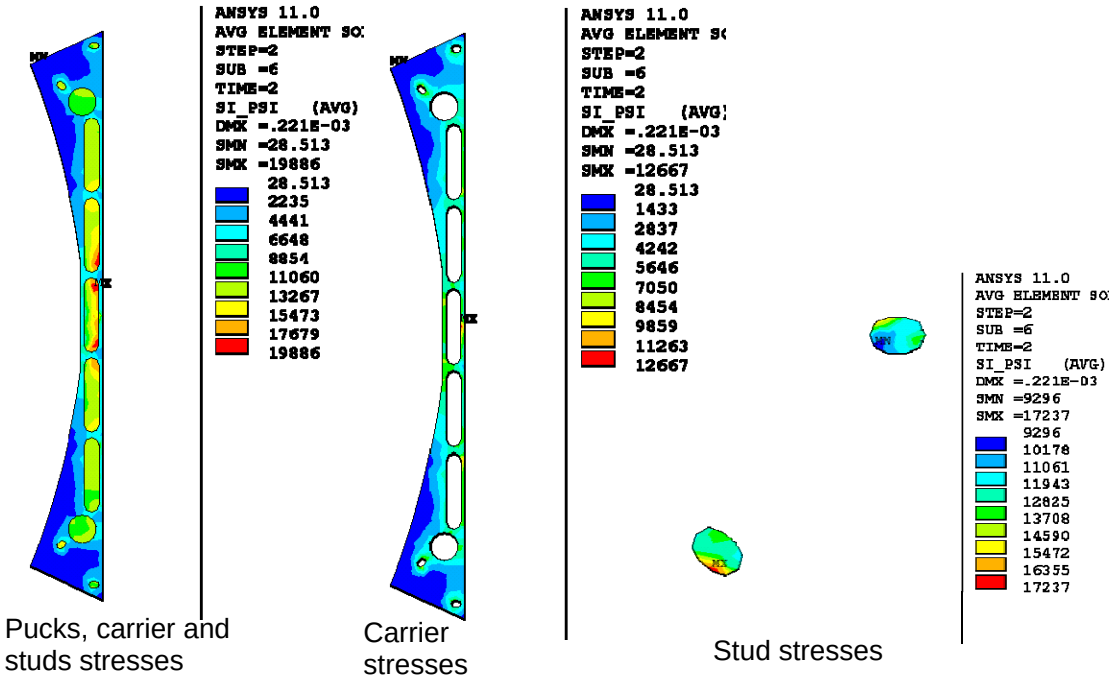

Fig. 20. Stress results for the inner leg compression assembly with outboard bolts.

Case #2: Bonded outboard leg with mu = 0.4 under the compression pucks.

In this run, the outboard bolts are removed and the flange is simply bonded between the flange and the shim. This reduces the computational solve time significantly. The inner pucks have a mu of 0.4 applied to their surfaces. Figure 21 shows the contact slip plot and the stress intensity for this scenario. The lower pucks do slip on one C flange and they transmit some shear as shown below. Since the pucks will slip, the pucks will likely eventually seat themselves against the edge of the carrier puck and transmit some amount of shear to the studs and other pucks which re still stuck. The fea model cannot address the possible wearing of the coating as it potentially slides over the flange surface. This dynamic effect should be evaluated by testing if possible but is not anticipated to be an issue for only 100,000 cycles of such localized motion

The peak stress (30 ksi) occurs in the studs and assumes that the studs are tightly secured to the carrier plate at all locations. The stress originates from two sources. The first source is from the relative stretching and movement of the C flange face compared to the carrier plate. The second source is from a small amount of shear stress which is transferred to the studs from the carrier plate.

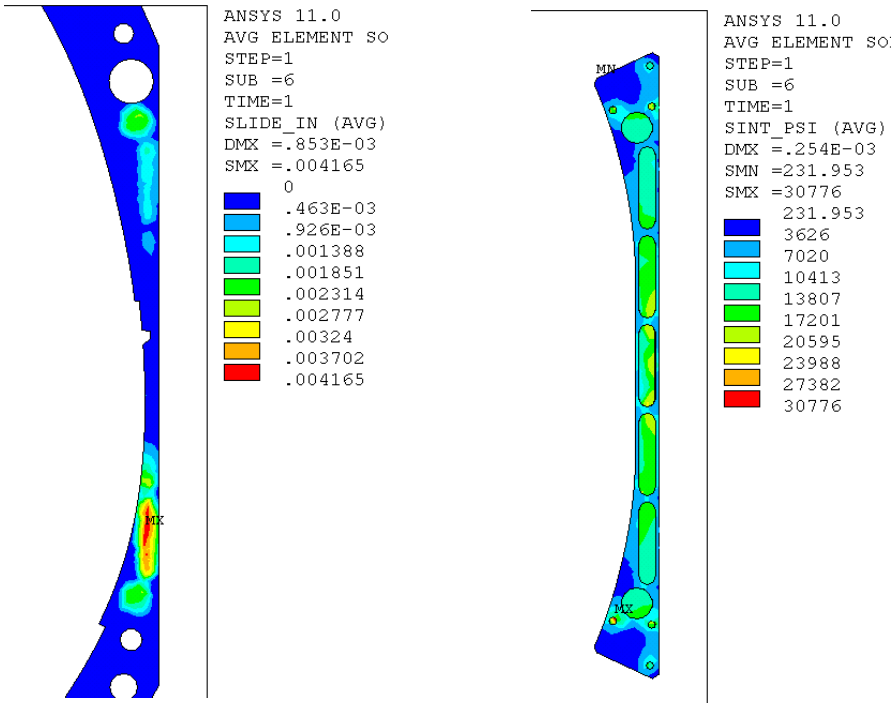

Puck sliding with mu = 0.4 Stress Intensity with mu = 0.4

Fig. 21. Sliding and stress intensity for bonded outboard leg and a friction coeffiecent of 0.4 between the compression pucks and the flange.

Case #3: Bonded outboard leg with mu = 0.4 under the compression pucks - No studs.

Since the studs may experience some shear if the pucks slide up against the carrier plate, this analysis determines if the inner pucks (which remained stuck in the previous runs) could react the shear if one side of the lower pucks slips. The outboard bolts are removed and the flange is simply bonded between the flange and the shim. The inner pucks have a mu of 0.4 applied to their surfaces but there are no studs in this model. Figure 22 shows the contact slip plot and the stress intensity for this scenario. The lower pucks do slip on one side and they transmit some shear to the other pucks which remain stuck. The compressive stress on the pucks is around 20 ksi and is similar to what is seen in the previous runs. Even with some relative scuffing of the lower alumina pucks, the inner pucks remain stuck and thus a mu of 0.4 is adequate to keep the pucks and carrier plate from dislodging from the C-C gap. The other noticeable difference here is that contact sliding has been reduced. This indicates that the carrier plate, which was attached to the flange through the studs in the previous two runs, is no longer being stretched and pulling the pucks with it. This is better explained in case #4 where the pucks ride on frictionless surfaces.

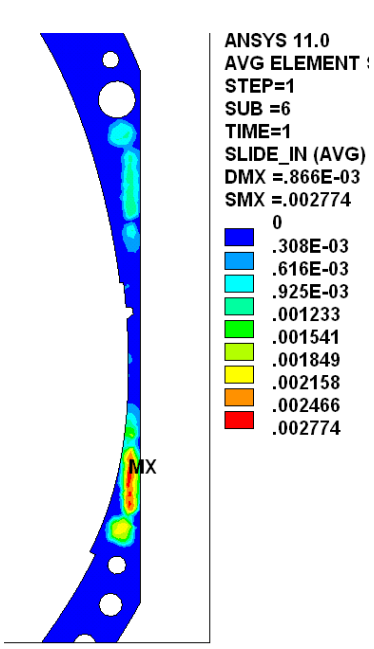

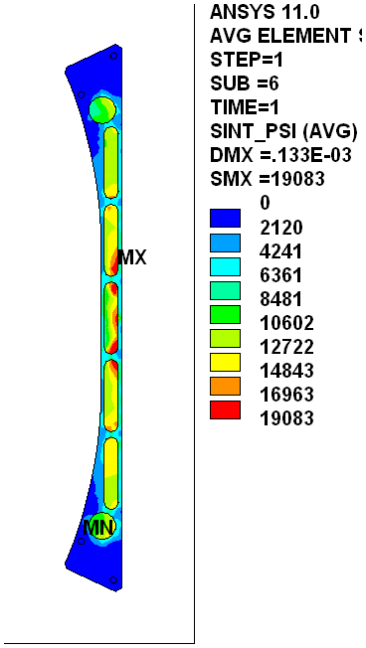

Puck sliding with mu = 0.4 Stress Intensity with mu = 0.4

Fig. 22. Sliding and stress intensity for bonded outboard leg and a friction coeffiecent of 0.4 between the compression pucks and the flange and no studs.

Case #4: Bonded outboard leg with mu = 0 under the compression pucks.

In this run, the outboard bolts are again removed and the flange is simply bonded between the flange and the shim. The inner pucks have a mu of 0.0 applied to their surfaces and the studs are in tight contact with the carrier plate. Figure 23 shows the contact slip plot and the stress intensity for this scenario. All of the pucks do slip on both surfaces and they are not able to transmit. The peak stress (25 ksi) occurs in the studs and assumes that the studs are tightly secured to the carrier plate at all locations. The stress on the studs is caused from the deformation of the CC flange surface under the carrier plate. The carrier plate is stretched and twisted by the motion of the C flange under EM loading. The carrier plate is constructed of stainless steel with alumina coating on all sides and thus is much stiffer than the weld studs which are being pulled by the C flange. Figure 24 shows the global deflection of the CC inner compression pucks/shims which indicates that the more massive C flange/casting is pulling the carrier plate and is loading the studs.

The peak stress and sliding values from the cases studied are shown in Table 6. These results indicate that the carrier plate should not be in tight contact with the studs. Doing so only increases the stress on the weld studs as the C flange will deform under magnetic loading (both vertically and in and out of plane). The other option is to use another softer material for the carrier plate. Further, the frictional surface (mu = 0.4) on the pucks is enough to keep the pucks near the midplane "stuck" even when the lower pucks slip when assuming that all pucks are in contact with the carrier (case # 3).

Table 6: Summary of Inner leg (unbolted region) results.

Case	outboard configuration	# of studs	puck contact friction	peak puck sliding (in)	peak puck stress (ksi)	peak stud stress (ksi)
1	bolts	2 oblong	zero	0.0057	19.9	17.2
2	bonded	3	0.4	0.0042	20.4	30.8
3	bonded	0	0.4	0.0027*	19	n/a
4	bonded	3	zero	0.0056	21	25
5	bonded	2	0.4	0.0044	21.3	39.2

* the lower slippage is from the lack of stud/carrier stretching.

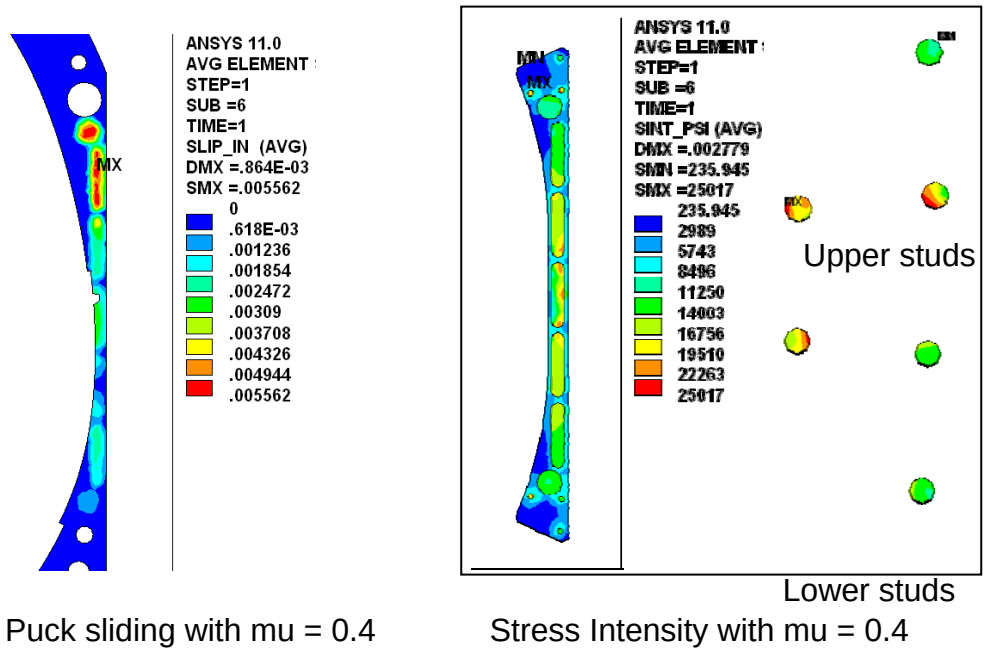

Fig. 23. Sliding and stress intensity for bonded outboard leg and a frictionlesss contact between the compression pucks and the flange.

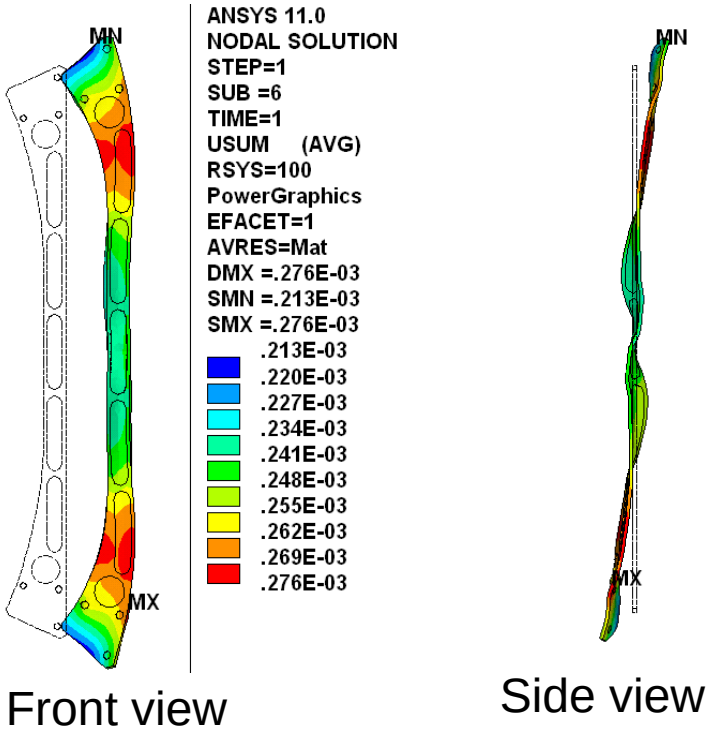

Fig. 24. Global Deflection of carrier for frictionless pucks (scaled by 500 X) with undefromed edge shape.

5. Summary

- 12 Added inboard bolts will reduce the motion of the inboard leg from .020” to less than .004”.
- All bolts remain “stuck” even when completely frictionless compression pucks are used on the inner legs.
- The lower compression pucks will slip slightly (< 0.004”) for a mu = 0.4 and may ride up against the carrier plate.
- Tight fitting studs experience the bulk of their stress form flange deformation relative to the carrier plate and only minimal shear is transferred to them when puck slippage occurs.
- The middle compression pucks will remain “stuck” even if there are no studs present. Thus, the shim plate will be restrained during operation with the slotted hole for stud design.

From the above list, loose fitting studs are preferable to tight fitting studs as this prevents the studs from experiencing any significant stress due to flange deformation. The slotted holes used near the studs in the design accomplish this by allowing the plate room to expand during EM loading. However, even in the worst case scenario, where the studs are in complete contact with the carrier plate, the peak stress (30 ksi) is still below the NCSX allowable average sm stress of 39.5 ksi. Currently, the deign calls for the carrier plate to be constructed of stainless steel and flame spayed with alumina. Since this plate will not see a compressive load and very little shear (from puck to puck, if one side slides relative to the other and the pucks are lined up against the carrier), a G11 carrier plate can also be considered. Finally, the friction coating in the puck sandwich should always be an alumina to stainless interface to ensure a coefficient of friction of at least 0.4 is maintained. Therefore, the pucks need to be coated on both sides.

References

[1] K.D.Freudenberg "Modular Coil Assembly Outboard Bolted Joint" NCSX-CALC-00-006, July 2007

[2] K.D.Freudenberg "Welded Joint FDR" NCSX-CALC-00-007, Nov 2007

[3] ANSYS Inc, 275 Technology Drive, Canonsburg, PA 15317

[4] K.D.Freudenberg "Non-Linear Modular Coil Analysis" NCSX-CALC-14-002-001, July 2007.

[5] Voght et al. "Low Temperature Fatigue of 316L and 316LN Austenitic Stainless Steels", Matallugical Transactions, March 14, 1990

[6] NCSX Specification: NCSX Structural Design Criteria, NCSX-Crit-Cryo Nov 2004.

[7] W.D. CAIN, "MAGFOR: A Magnetics Code to Calculate Field and Forces in Twisted Helical Coils of Constant Cross-Section", 10th IEEE/NPSS Symposium on Fusion Engineering, 1983

[8] H.M. Fan. "Nonlinear Analysis of Modular Coil and Shell Structure" NCSX-CALC-14-001-001, February 2006

A.1 Using Larger C-C inner Leg Bolts

CC Connection with 1.5” bolts

NCSX NATIONAL COMPACT STELLARATOR EXPERIMENT

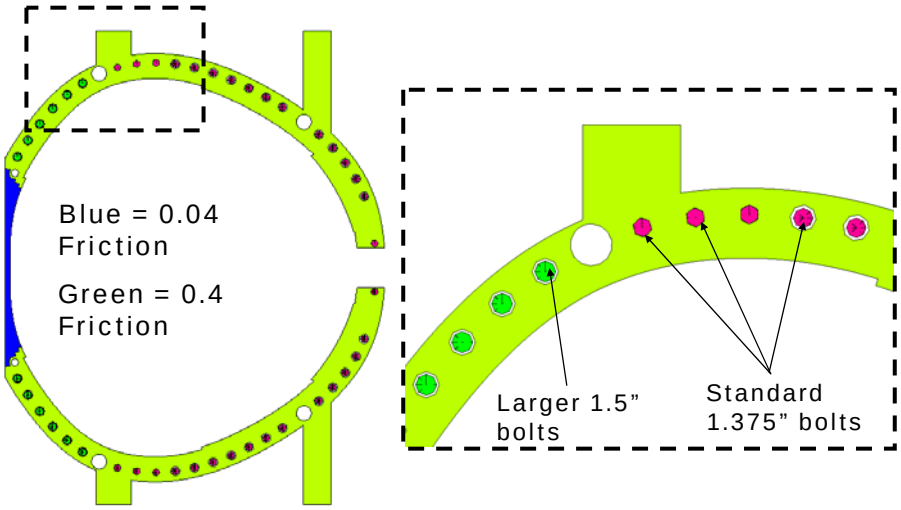

1.5” bolts will have approximately 90 Kips preload or 20% increase from 1.375” bolts.

6 ADDED 1.5” BOLTS

NCSX NATIONAL COMPACT STELLARATOR EXPERIMENT

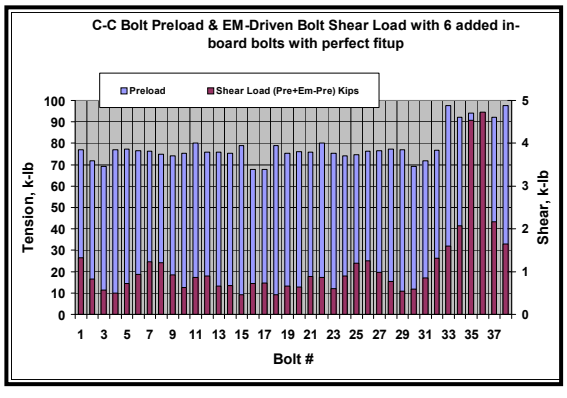

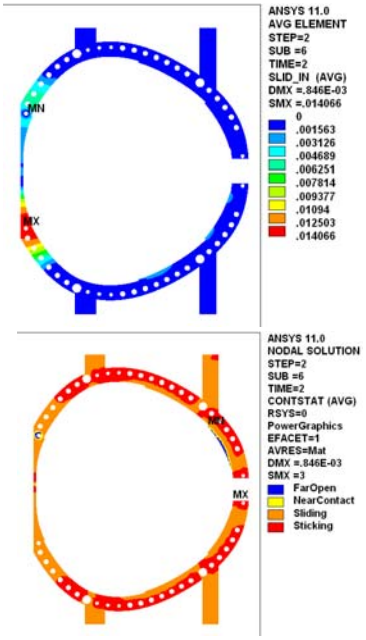

Friction = 0.04 on Inner-leg region, mu = 0.4 everywhere else

Outer Bolts #1 and #32 are now completely stuck. Inner leg slippage has been essentially eliminated.

Innermost inboard bolts (#35 - #36) are stuck according to the status plot.

12 ADDED 1.5” BOLTS

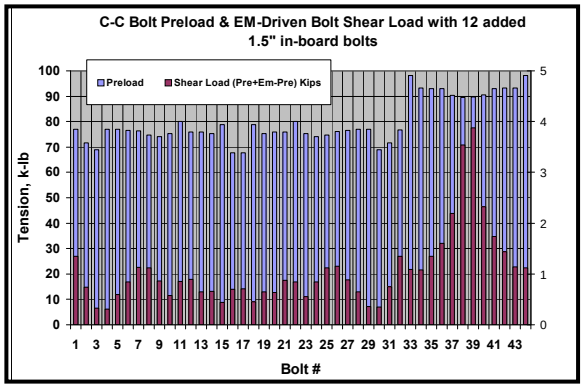

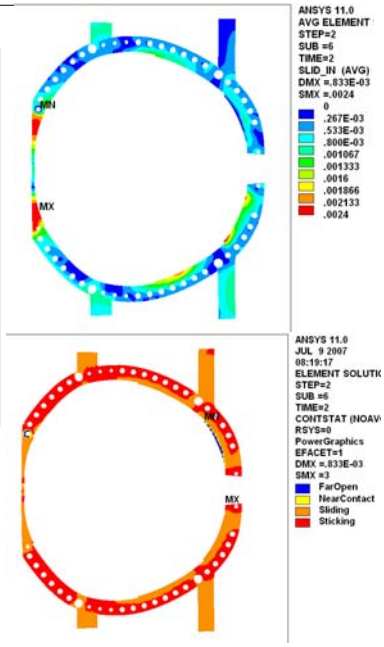

Friction = 0.04 on Inner-leg region, mu = 0.4 everywhere else

Outer Bolts #1 and #32 are now completely stuck. Inner leg slippage has been essentially eliminated.

Innermost inboard bolts (#38 - #39) are still stuck.

Three Innermost Bolts Added

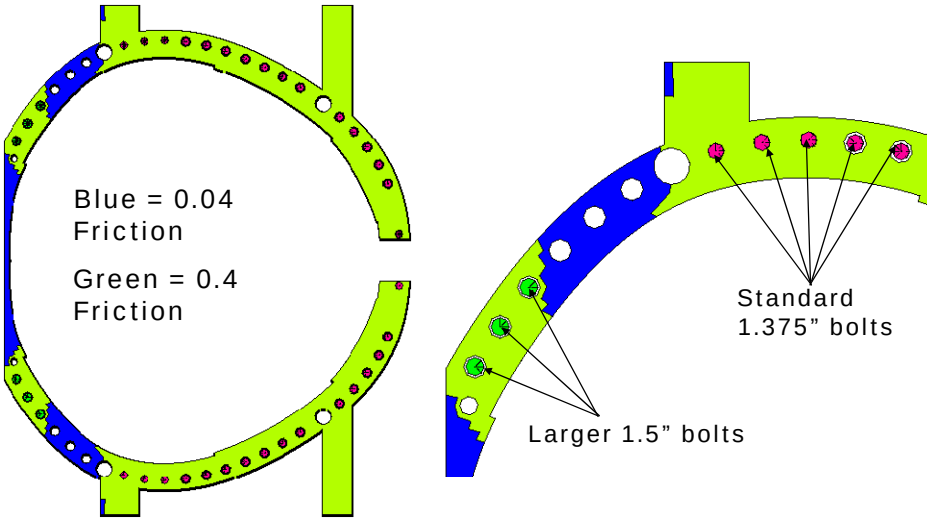

Reverse 6 ADDED 1.5” BOLTS

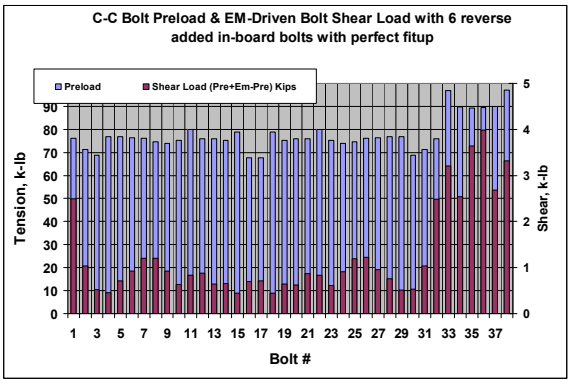

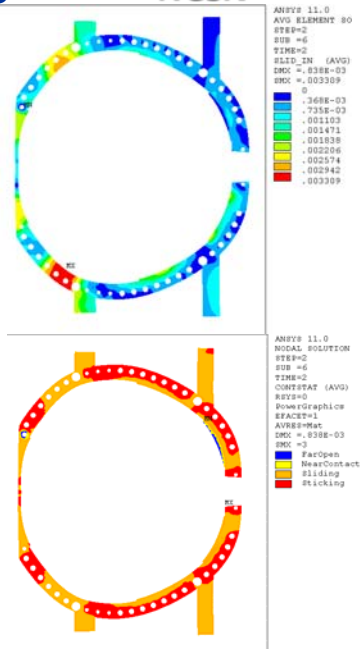

Friction = 0.04 on Inner-leg region,
mu = 0.4 everywhere else

Outer Bolts #1 and #32 are now completely stuck.
Inner leg slippage has been essentially eliminated.

Innermost inboard bolts (#35 - #36) are still stuck.

Study on the Inner Leg of CC

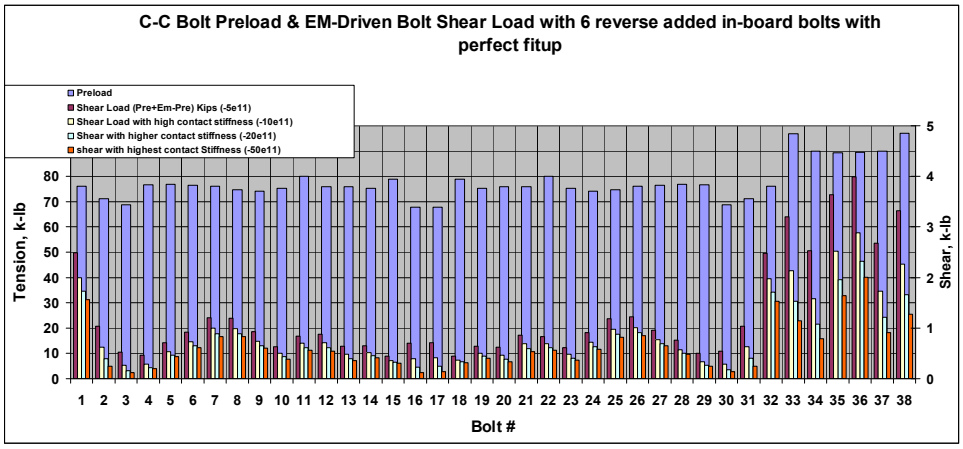

Inner Leg Bolts Only

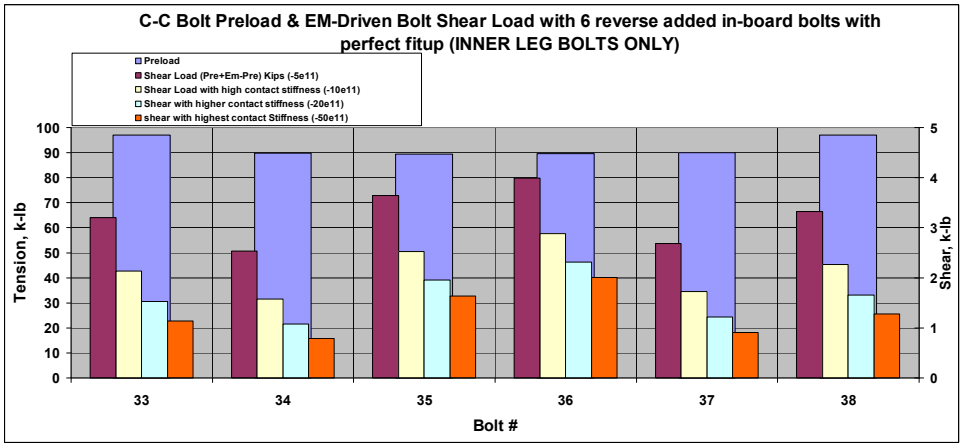

A.2 Previous studies on the inner leg shear and compression.

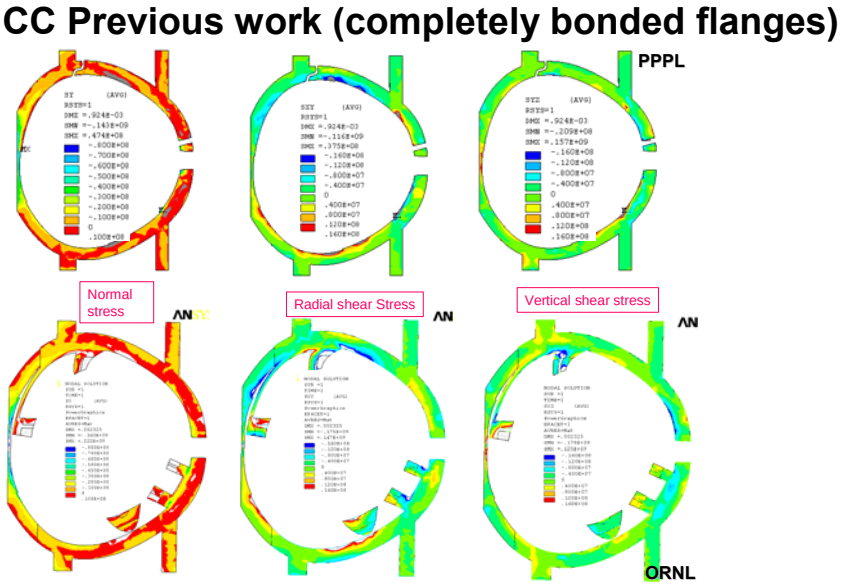

As shown in the first picture form the left, the compressive stress is largest near the midplane, This has all of the available area taking the compression.